TABLE I. ADAMTS 13 and its Inhibitory Activity During Different Phases of Cyclosporine Therapy in Resistant/Relapsed TTP Patients

No. patients	ADAMTS 13 activity at the beginning of cyclosporine	Presence of anti-ADAMTS 13 auto-antibodies	ADAMTS 13 activity at response	Presence of anti-ADAMTS 13 auto-antibodies at response	Relapse	ADAMTS 13 activity at relapse	Presence of anti-ADAMTS 13 auto-antibodies at relapse
1	<5%	+	30%	Negative	After reduction of cyclosporine dosage	<5%	Negative
2	<5%	+−	60%	Negative	NO (after cyclosporine suspension)		
3	<5%	+++	<5%	+++	During cyclosporine treatment	<5%	+++
4	<5%	++	<5%	++	During cyclosporine treatment	<5%	++
5	<5%	+++	100%	Negative	After reduction of cyclosporine dosage (new response to correct dosage)	<5%	++
6	<5%	Not done	72%	Negative	NO		
7	<5%	+	93%	Negative	NO		

References

1. Kappers-Klunne MC, Wijemans P, Fijnheer R, et al. Splenectomy for the treatment of thrombotic thrombocytopenic purpura. Br J Haematol 2005;130:768–776.
2. Garvey B. Rituximab in the treatment of autoimmune haematological disorders. Br J Haematol 2008;141:149–169.
3. Cataland SR, Jin M, Lin S, et al. Effect of prophylactic cyclosporine therapy on ADAMTS 13 biomarkers in patients with idiopatic thrombotic thrombocytopenic purpura. Am J Hematol 2008;83:911–915.
4. Peyvandi F, Lavoretano S, Palla R, et al. ADAMTS 13 and anti-ADAMTS 13 antibodies as markers for recurrence of acquired thrombotic thrombocytopenic purpura during remission. Haematologica 2008;93:232–239.
5. Nosari A, Bernuzzi P, Corneo R, et al. Late response to cyclosporine in refractory thrombotic thrombocytopenic purpura. Int J Hematol 2002;76:284–286.
6. Doldan-Silvero A, Acevedo-Gadea C, Habib C, et al. ADAMTS 13 activity and inhibitor. Am J Hematol 2008;83:811–814.

Clinical efficacy of WT1 peptide vaccination in patients with acute myelogenous leukemia and myelodysplastic syndrome

To the editor: Because Wilms tumor antigen 1 (WT1) is preferentially expressed in various kinds of malignancies including acute leukemia but not normal cells, investigators are attempting to develop cellular immunotherapy for cancers targeting WT1 [1–6]. We previously identified the WT1-derived peptide that can be recognized by HLA-A*2402-restricted cytotoxic T lymphocytes (CTLs) and elicit leukemia-reactive CTLs [7–9]. A phase I clinical study of a cancer vaccine using this WT1 peptide is currently underway in our hospital. Here we report two interesting cases in which a clinical effect of WT1 peptide vaccination was detected.

The first case is chemotherapy-resistant acute myelogenous leukemia (AML) (Fig. 1A). A 72-year-old woman with de novo AML (M2) received the standard induction chemotherapy with daunorubicin and cytarabine and achieved complete remission. After 2 years, her AML relapsed and reinduction chemotherapy was performed, again resulting in complete remission. However, the AML relapsed again after 6 months, and low-dose cytarabine was administered. After this treatment, the bone marrow was normocellular, with 7% leukemic cells. The patient was then enrolled in the Phase I clinical study of WT1 peptide vaccination, as reviewed and approved by the Institutional Review Board of Ehime University Hospital. She received subcutaneous injection of 1 mg $WT1_{235\text{-}243}$ (CMTWNQMNL) peptide in Montanide adjuvant biweekly, and the WT1 peptide vaccine was administered totally 20 times. After the 5th vaccination, an aspirated bone marrow sample showed hypoplasia with less than 3% myeloblasts. The patient has since been followed up for more than 3 years. Pancytopenia and hypoplasia of the bone marrow without an increase of myeloblasts have persisted during this observation period.

The second case is a 55-year-old male with myelodysplastic syndrome (MDS) that had evolved from aplastic anemia (Fig. 1B). Despite intensive therapies, pancytopenia had persisted, and the patient had been receiving red blood cell transfusion frequently when his hemoglobin level fell to less than 6.0 g/dL. When this patient was enrolled in the WT1 peptide vaccine trial, bone marrow aspiration revealed normoplasia with 2.2% myeloblasts and a slightly increased expression level of WT1 mRNA. After vaccination with 1 mg WT1 peptide, the hemoglobin level gradually increased and the WT1 mRNA level in bone marrow cells decreased to within the normal range. The patient was vaccinated with WT1 peptide totally 30 times, and has been followed up for more than 3 years. His hemoglobin level has been maintained at more than 7.0 g/dL, and no red blood cell transfusion has been required during WT1 peptide vaccination.

The data of $WT1_{235\text{-}243}$/HLA-A*2402 tetramer assay for monitoring WT1-specific CTLs was shown in Fig. 2. Since we could not detect WT1-specific CTLs apparently when freshly isolated lymphocytes were used for assays, peripheral blood mononuclear cells were stimulated with $WT1_{235\text{-}243}$ peptide in vitro and then analyzed. WT1-specific CTLs were not detected in peripheral blood of both patients before WT1 peptide vaccination, and were apparently detected after the 3rd or 4th vaccination. $WT1_{235\text{-}243}$-specific CTL lines were generated by stimulation of peripheral blood lymphocytes from these patients with WT1 peptide in vitro (data not shown).

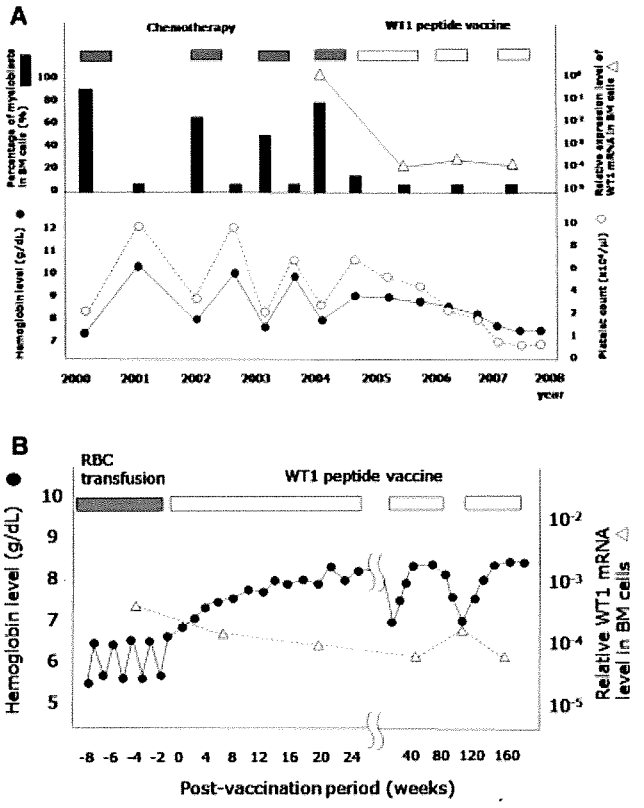

Fig. 1. Clinical efficacy of WT1 peptide vaccination. (A) Clinical course of the patient with AML. Pancytopenia and hypoplasia of bone marrow occurred, but the leukemia cells did not proliferate after WT1 peptide vaccination. (B) Clinical course of the patient with MDS. The hemoglobin level increased gradually after WT1 peptide vaccination and decreased during discontinuance of vaccination.

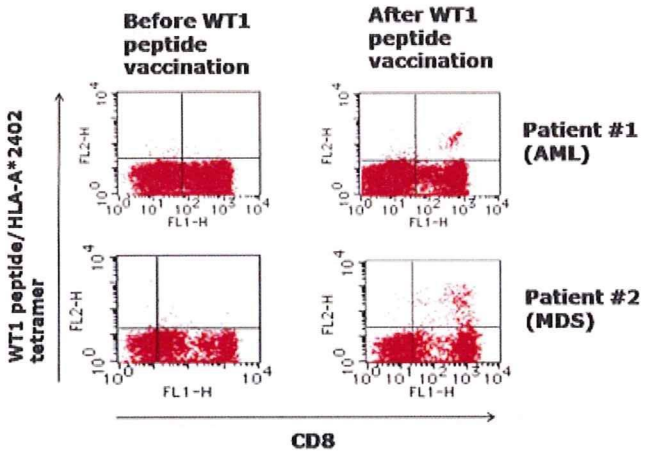

Fig. 2. Tetramer assays for detection of $WT1_{235-243}$-specific CTLs. Peripheral blood mononuclear cells isolated from the patients were stimulated with $WT1_{235-243}$ peptide in vitro and then stained with $WT1_{235-243}$/HLA-A*2402 tetramer. WT1-specific CTLs were detected in peripheral blood of the patients after WT1 peptide vaccination. [Color figure can be viewed in the online issue, which is available at www.interscience.wiley.com.]

In the first patient with AML, pancytopenia was developed following WT1 peptide vaccination. The hypothesis that normal hematopoietic stem cells as well as leukemia cells were also damaged by WT1-specific CTLs seems unlikely to be by the following reasons. The first is that WT1-specific CTLs were increased after the 5th vaccination resulting in the decrease of myeloblasts, but at this time normal hematopoiesis was not significantly damaged. The second reason is that the other clinical studies using WT1 peptide vaccination showed that WT1-specific CTLs did not damage normal hematopoiesis. One of the possibilities is that this AML case might have a component of MDS and that WT1-expressing transformed stem cells, from which erythrocytes and platelets were derived, were damaged by WT1-specific CTLs, resulting in pancytopenia as reported previously in a case of MDS-derived AML [10]. The mechanism responsible for the improvement of anemia in the second patient with MDS is unclear, but it is speculated that WT1-specific CTLs may have lysed abnormal clone cells that had inhibited normal hematopoiesis. Taken together with papers previously published [2,3,5,10], our data indicate that immunotherapy targeting WT1 might be promising; however, precise monitoring of hematopoiesis in vaccinated patients is important.

Masaki Yasukawa[1]
Hiroshi Fujiwara[1]
Toshiki Ochi[1]
Koichiro Suemori[1]
Hiroshi Narumi[1]
Taichi Azuma[1]
Kiyotaka Kuzushima[2]

[1]*Department of Bioregulatory Medicine, Ehime University Graduate School of Medicine, Ehime, Japan*
[2]*Division of Immunology, Aichi Cancer Center, Nagoya, Aichi, Japan*

Published online 19 February 2009 in Wiley InterScience (www.interscience.wiley.com).
DOI: 10.1002/ajh.21387

References

1. Xue S, Gao L, Gillmore R, et al. WT1-targeted immunotherapy of leukaemia. Blood Cells Mol Dis 2004;33:288–290.
2. Oka Y, Tsuboi A, Taguchi T, et al. Induction of WT1 (Wilms' tumor gene)-specific cytotoxic T lymphocytes by WT1 peptide vaccine and the resultant cancer regression. Proc Natl Acad Sci USA 2004;101:13885–13890.
3. Mailänder V, Scheibenbogen C, Thiel E, et al. Complete remission in a patient with recurrent acute myeloid leukemia induced by vaccination with WT1 peptide in the absence of hematological or renal toxicity. Leukemia 2004;18:165–166.
4. May RJ, Dao T, Pinilla-Ibarz J, et al. Peptide epitopes from the Wilms' tumor 1 oncoprotein stimulate $CD4^+$ and $CD8^+$ T cells that recognize and kill human malignant mesothelioma tumor cells. Clin Cancer Res 2007;13:4547–4555.
5. Rezvani K, Yong AS, Mielke S, et al. Leukemia-associated antigen-specific T-cell responses following combined PR1 and WT1 peptide vaccination in patients with myeloid malignancies. Blood 2008;111:236–242.
6. Kitawaki T, Kadowaki N, Kondo T, et al. Potential of dendritic cell immunotherapy for relapse after allogeneic hematopoietic stem cell transplantation, shown by WT1 peptide- and keyhole limpet hemocyanin-pulsed, donor-derived dendritic cell vaccine for acute myeloid leukemia. Am J Hematol 2008;83:315–317.
7. Ohminami H, Yasukawa M, Fujita S. HLA class I-restricted lysis of leukemia cells by a $CD8^+$ cytotoxic T-lymphocyte clone specific for WT1 peptide. Blood 2000;95:286–293.
8. Azuma T, Makita M, Ninomiya K, et al. Identification of a novel WT1-derived peptide which induces human leucocyte antigen-A24-restricted anti-leukaemia cytotoxic T lymphocytes. Br J Haematol 2002;116:601–603.
9. Makita M, Hiraki A, Azuma T, et al. Antilung cancer effect of WT1-specific cytotoxic T lymphocytes. Clin Cancer Res 2002;8:2626–2631.
10. Oka Y, Tsuboi A, Murakami M, et al. Wilms tumor gene peptide-based immunotherapy for patients with overt leukemia from myelodysplastic syndrome (MDS) or MDS with myelofibrosis. Int J Hematol 2003;78:56–61.

Effective treatment for *de novo* hepatitis B with nucleotide analogue in patients with hematological malignancies

To the editor: Individuals with resolved hepatitis B, characterized as hepatitis B surface antigen (HBsAg)-negative and hepatitis B core antibody (anti-HBc)-positive, have latent hepatitis B virus (HBV) infection in their liver tissue [1–3]. Cytotoxic chemotherapy and hematopoietic stem cell transplantation sometimes trigger the reactivation of latently infected HBV, resulting in *de novo* hepatitis B [4–6]. Although *de novo* hepatitis B could cause acute liver failure or chronic hepatitis, an effective management strategy for *de novo* hepatitis B has not been well established. The benefit of prophylactic antiviral therapy to HBsAg-negative but anti-HBc-positive patients remains controversial, because HBV activation is infrequent and there is not enough information to recommend routine prophylaxis at this time [7,8]. We report two patients of *de novo* hepatitis B after treatment for malignant lymphoma who were treated by nucleotide analogues. Nucleotide analogue treatment immediately after the occurrence of *de novo* hepatitis B resolved the hepatitis and induced clearance of serum HBsAg and HBV DNA in both patients. Notably, both patients remained negative for HBsAg and HBV DNA in their serum even after termination of nucleotide analogue treatment.

Patient 1. A 62-year-old man first presented with abdominal pain. Gastroscopy showed an ulcerative lesion at the fornix of the stomach. An endoscopic biopsy of the ulcerative lesion showed diffuse large B cell lymphoma. He was treated with six cycles of EPOCH chemotherapy (etoposide, prednisolone, vincristine, cyclophosphamide, and doxorubicin) with rituximab followed by one course of R-CHOP chemotherapy (rituximab, cyclophosphamide, adriamycin, vincristine, and prednisolone) and then received autologous peripheral blood stem cell transplantation (auto-PBSCT) 10 months after diagnosis. He achieved complete remission.

Before auto-PBSCT, he was negative for HBsAg but positive for hepatitis B surface antibody (anti-HBs) and anti-HBc. After auto-PBSCT, we again confirmed that he was negative for HBsAg and hepatitis Be antigen (HBeAg) but positive for anti-HBs and anti-HBc. A sensitive polymerase chain reaction assay revealed no evidence of HBV DNA in his serum. Although his serum alanine aminotransferase (ALT) level was within normal limits until 8 months after auto-PBSCT, it increased to 252 IU/ml during the next month. Coincident with the elevation of ALT level, he became positive for HBsAg and HBeAg but negative for anti-HBs. At that stage, his serum HBV DNA level was $10^{7.3}$ copies/ml. He was diagnosed with *de novo* hepatitis B and lamivudine therapy (100 mg/day) was started 7 days after the elevation in ALT. Twenty-nine days after the initiation of lamivudine treatment, he was negative for HBsAg and his serum level of HBV DNA had decreased to $10^{4.6}$ copies/ml. After 105 days of lamivudine treatment, serum HBV DNA was undetectable and he was negative for HBeAg. Because he acquired anti-HBs and hepatitis Be antibody (anti-HBe) in his serum, lamivudine treat-

Cancer Immunity (1 October 2009) Vol. 9, p. 8
Submitted: 4 August 2009. Accepted: 10 September 2009.

CANCER
IMMUNITY
Article

Correlation of high and decreased NY-ESO-1 immunity to spontaneous regression and subsequent recurrence in a lung cancer patient

Midori Isobe[1], Shingo Eikawa[1], Akiko Uenaka[1], Yoichi Nakamura[2], Tetsuo Kanda[3], Shigeru Kohno[2], Kiyotaka Kuzushima[4] and Eiichi Nakayama[1]

[1]*Department of Immunology, Okayama University Graduate School of Medicine, Dentistry and Pharmaceutical Sciences, Okayama, Japan*
[2]*Department of Medicine, Nagasaki University School of Medicine, Nagasaki, Japan*
[3]*Department of Internal Medicine, Goto Central Hospital, Goto, Japan*
[4]*Department of Immunology, Aichi Cancer Center, Nagoya, Japan*

Communicated by: LJ Old

We show correlation between strong and decreased NY-ESO-1-specific immunity with spontaneous regression and subsequent recurrence, respectively, in a long-surviving patient with an NY-ESO-1-expressing lung adenocarcinoma. An integrated immune response consisting of IgG antibody, as well as CD4 and CD8 T cells, against NY-ESO-1 was observed at the time of spontaneous regression of multiple pleural metastases. After tumor dormancy for 3 years, the tumor started to progress. IgG antibody levels and the number of CD4 and CD8 T cells against NY-ESO-1 decreased, but were still detectable. On the other hand, the number of Foxp3+ CD25 high T regulatory cells gradually increased. The findings suggest the relevance of the NY-ESO-1 immune response and its regulation by Foxp3+ CD25 high T regulatory cells in the clinical course of this lung cancer patient.

Keywords: human, lung cancer, NY-ESO-1, humoral immunity, cellular immunity

Introduction

The NY-ESO-1 antigen was originally found in an esophageal cancer by serological recombinant cDNA expression cloning (SEREX) and is in the category of cancer/testis (CT) antigens (1-3). Its expression is restricted to germ cells in the testes in normal adult tissues, but is observed in various cancer types at different frequencies (4). A characteristic of the NY-ESO-1 antigen is its extremely high immunogenicity (5). Patients with NY-ESO-1-expressing tumors frequently show a spontaneous immune response to the NY-ESO-1 antigen. An antibody response against the NY-ESO-1 antigen was frequently observed in patients with NY-ESO-1-expressing tumors (6, 7). Most patients who showed an antibody response also showed CD4 and CD8 T cell responses (8, 9). Such strong immunogenicity indicates the NY-ESO-1 antigen to be a very promising candidate target molecule for a cancer vaccine.

We recently reported a lung adenocarcinoma patient who showed spontaneous regression of multiple pleural metastases without any treatment (10). Analysis of the immune response using the patient's peripheral blood revealed extremely strong immune responses to the NY-ESO-1 antigen, but not to other CT antigens commonly expressed in lung cancer in the Japanese population. Recently, the patient showed tumor recurrence. In this paper, we show a correlation between high and decreased NY-ESO-1-specific immunity to spontaneous regression and subsequent recurrence. A gradual decrease in NY-ESO-1 immunity was associated with a gradual increase in regulatory T cells (Tregs), suggesting the relevance of Tregs for recurrent tumor progression.

Results

Spontaneous regression and recurrence of the lung adenocarcinoma in patient GO

Patient GO is a 71-year old Japanese man. A right hilar tumor (3 x 3 cm) and right multiple pleural tumors were found by chest computed tomography in November 2004 (10). The hilar tumor was unchanged, but the pleural metastases regressed spontaneously by March 2005. Histopathological examination of pleural metastases biopsy specimens showed that the tumor was a poorly differentiated adenocarcinoma. Immunohistochemical analyses showed that approximately 50%-60% of the tumor cells expressed NY-ESO-1 and 30%-40% expressed HLA class I antigens. Infiltration by many CD8 T cells was observed in the stromal tissue surrounding the tumor and in the tumor tissue. Subsequently, a tumor was noticed in the right lower lobe in November 2007 (Figure 1 and Figure 2A) that was probably the primary lesion which had disappeared and left a scar by his first visit to the hospital in November 2004. The tumors gradually increased in size until April 2009.

Serum antibody response

The serum antibody response against CT antigens, whose expression is frequently observed in lung cancer, was investigated in patient GO using recombinant proteins by ELISA. An antibody against NY-ESO-1, but not against XAGE-1b, SSX2 or SSX4, was observed (10). An extremely strong serum IgG response against NY-ESO-1 was observed from March 2005 to July 2006 during the course of the disease (Figure 2). Thereafter, the response decreased gradually. The serum IgM response decreased gradually from March 2005 onwards and was undetectable in July 2006. The dominant IgG subtype was IgG1 (Figure 2C).

Figure 1

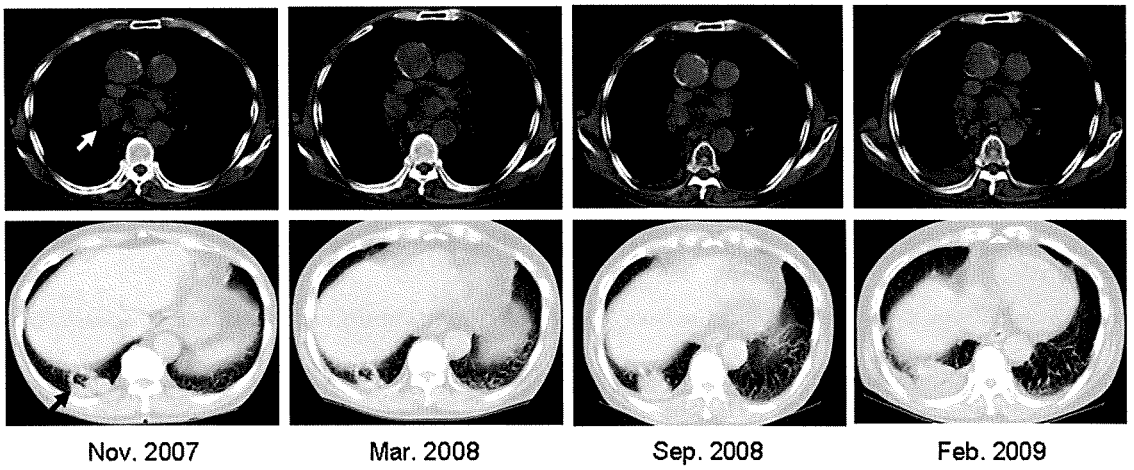

Chest computed tomography. The white arrow indicates a right hilar tumor of the lung and the black arrow indicates a new lesion in the right lower lobe.

Figure 2

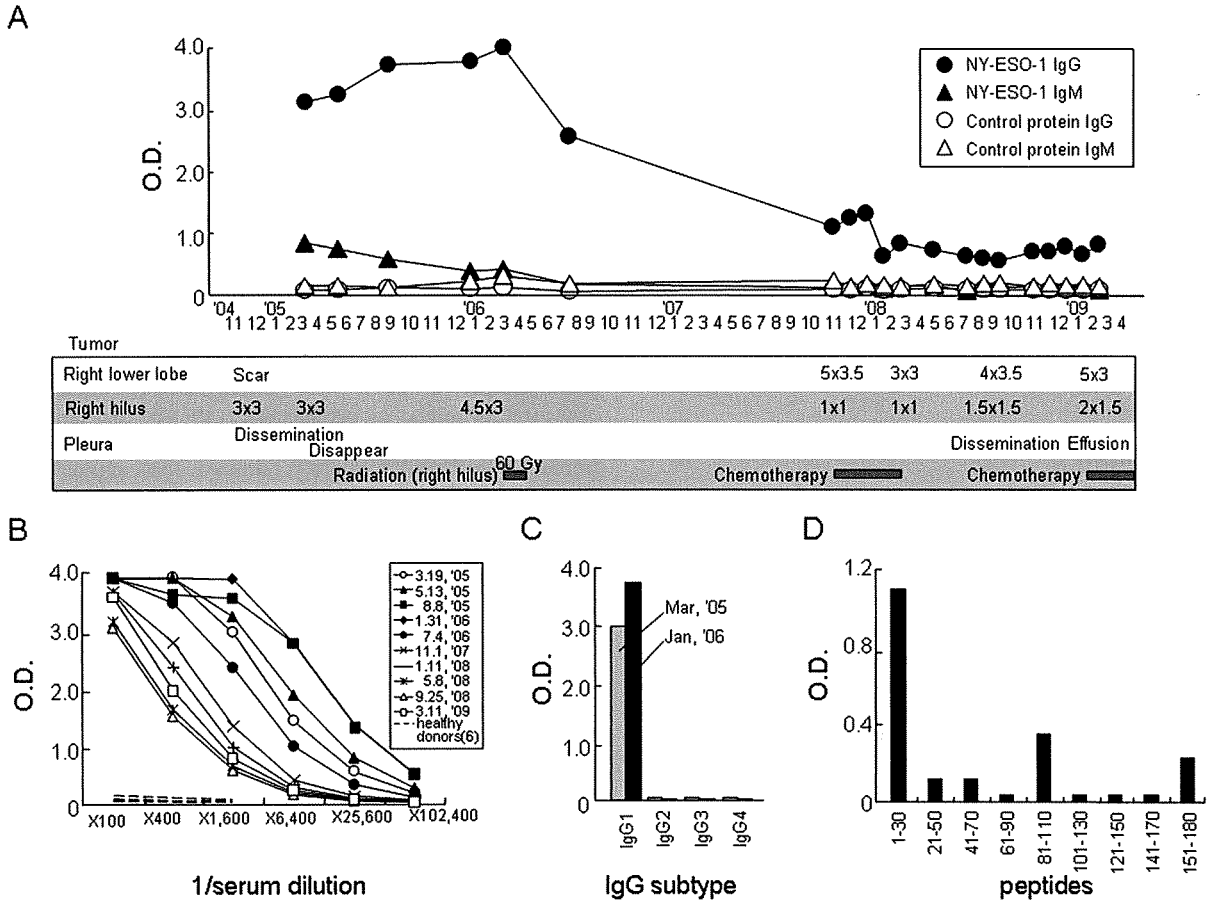

Serum antibody response against NY-ESO-1 in patient GO. (A) The IgG and IgM responses against recombinant NY-ESO-1 protein at a serum dilution of 1:1,600 were plotted during the course of the disease. The control recombinant protein used was RL-Akt. The clinical course and treatments shown in the box correspond to the time points. (B) Titration of serum obtained at different time points is shown. Sera from 6 healthy donors were included as a control. (C) The IgG subtype was determined using specific secondary mAbs for detection. (D) The peptide regions recognized by the antibody were determined using 30-mer NY-ESO-1 overlapping peptides.

Figure 3

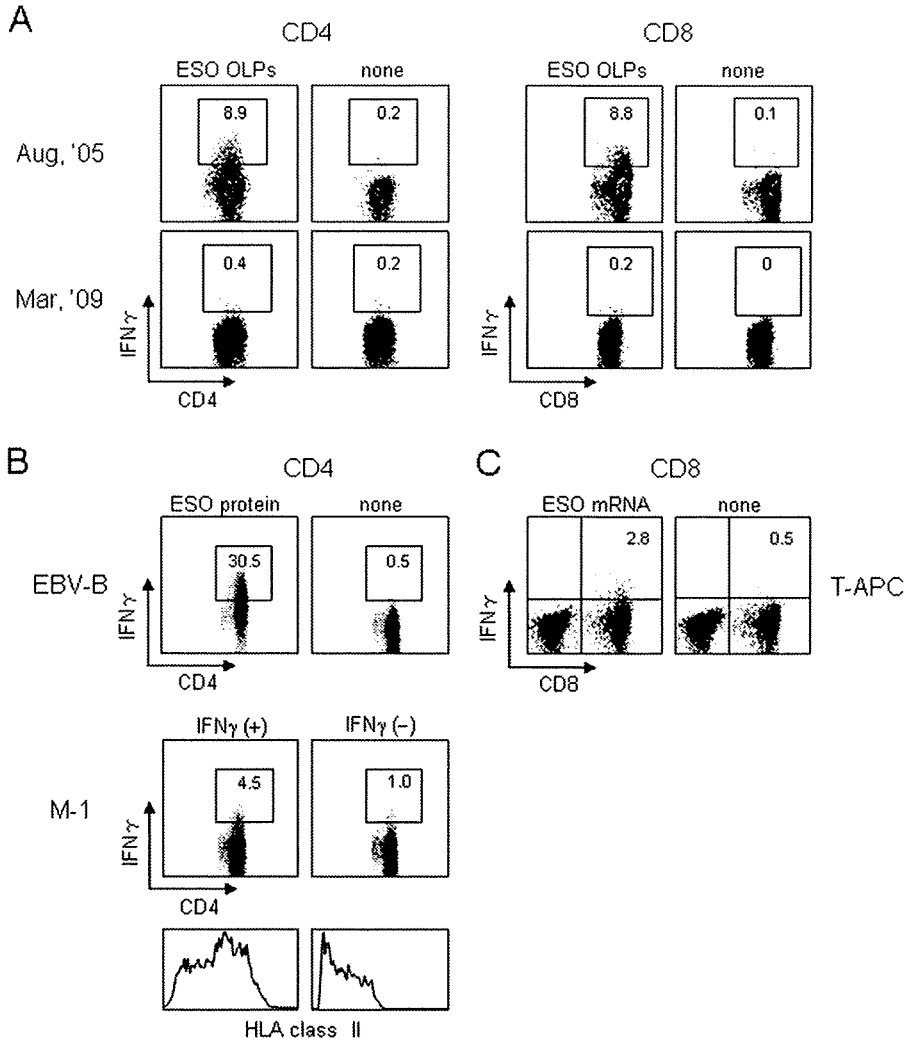

IFNγ secretion assays. MACS beads-purified CD4 and CD8 T cells (2×10^6) from PBMCs were cultured with irradiated (40 Gy) autologous CD4- and CD8-depleted PBMCs (2×10^6) as APCs in the presence of 28 overlapping 18-mer peptides and a 30-mer C-terminal peptide (OLPs) spanning the entire NY-ESO-1 protein (1 μg of each peptide/ml) in 24-well culture plates for 12 days. (A) IFNγ secretion by CD4 and CD8 T cells (1×10^5) was assayed against PFA-treated CD4- and CD8-depleted PBMCs (1×10^5) pre-pulsed with NY-ESO-1 OLPs for 30 min. (B and C) CD4 and CD8 T cells obtained in August 2005 were used on the twenty-sixth day following two stimulations. (B) IFNγ secretion by CD4 T cells (1×10^5) was assayed against the patient's EBV-transformed B cells (1×10^5) pretreated with NY-ESO-1 protein (20 μg/ml) for 24 h, and NY-ESO-1-expressing melanoma (M-1) cells (1×10^5) pretreated with IFNγ (100 U/ml) for 48 h by stimulation for 4 h. HLA class II expression on M-1 cells after IFNγ treatment is also shown. (C) IFNγ secretion by CD8 T cells (1×10^5) was assayed against the patient's PHA-stimulated CD4 T cells (T-APC) (1×10^5) transfected with *NY-ESO-1* mRNA (20 μg).

The peptide regions recognized by the antibody were defined using 30-mer overlapping peptides spanning the entire NY-ESO-1 protein. A peptide corresponding to amino acids 1-30 was the region dominantly recognized by the antibody (Figure 2D), while peptides corresponding to amino acids 81-110 and 151-180 were weakly recognized.

CD4 and CD8 T cell responses and their recognition of NY-ESO-1 peptides

CD4 and CD8 T cell responses against NY-ESO-1 in patient GO were investigated by an IFNγ secretion assay using 28 18-mer overlapping peptides and a 30-mer C-terminal peptide (OLPs) spanning the entire NY-ESO-1. MACS beads-purified CD4 and CD8 T cells from PBMCs were cultured with irradiated (40 Gy) autologous CD4- and CD8-depleted PBMCs as APCs in the presence of a mixture of OLPs for 12 days. The cells were then assayed for IFNγ secretion against paraformaldehyde (PFA)-fixed autologous CD4- and CD8-depleted PBMCs pre-pulsed with OLPs. As shown in Figure 3, extremely strong CD4 and CD8 T cell responses were observed in PBMCs obtained in August 2005 when the strong IgG response was observed. On the other hand, decreased CD4 and CD8 T cell responses were observed in PBMCs obtained in March 2009, when a decreased IgG response was observed. After two *in vitro* stimulations, however, significantly amplified CD4 and CD8 T cell responses were detected in PBMCs obtained in March 2009 (data not shown), confirming the

Figure 4

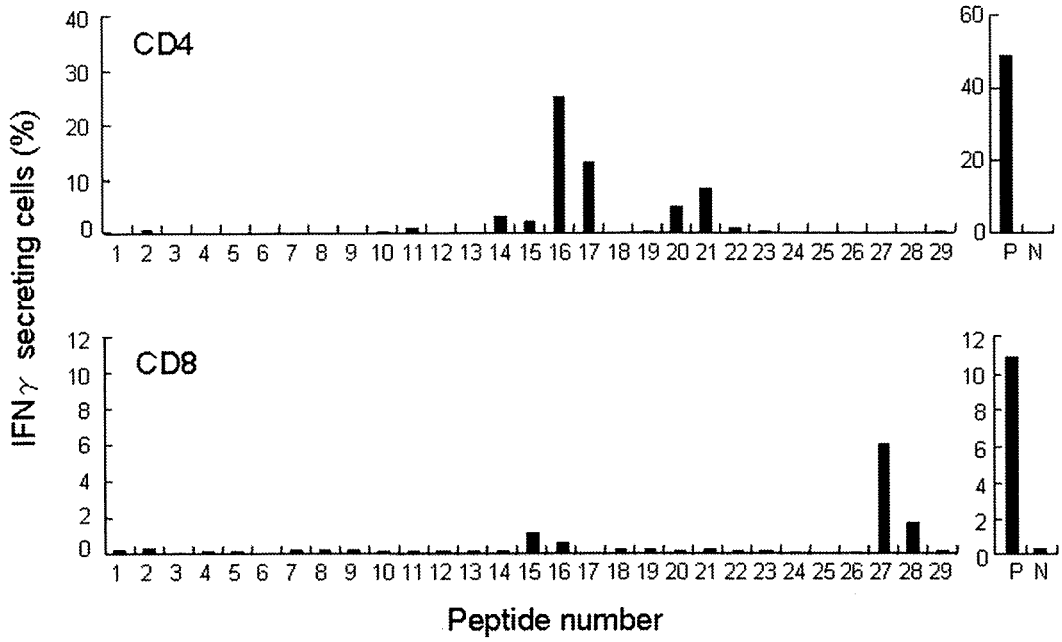

NY-ESO-1 regions recognized by CD4 and CD8 T cells in patient GO. MACS beads-purified CD4 and CD8 T cells (2×10^6) from PBMCs obtained in August 2005 were cultured with irradiated (40 Gy) autologous CD4- and CD8-depleted PBMCs (2×10^6) as APCs in the presence of 28 overlapping 18-mer peptides and a 30-mer C-terminal peptide (OLPs) at a concentration of 1 μg/ml of each peptide in a 24-well culture plate for 14 days. On the twenty-sixth day after two stimulations, CD4 and CD8 T cells (3×10^4) were assayed for IFNγ secretion against PFA-treated autologous CD4- and CD8-depleted PBMCs (3×10^4) pre-pulsed with the individual peptide after stimulation for 4 h. The peptide number corresponds to the individual overlapping peptides. Abbreviations: P, positive control stimulated with a mixture of OLPs; N, negative control without peptides.

presence of specific CD4 (0.2%) and CD8 (0.2%) T cells in the assay stimulated once *in vitro*.

The response of CD4 T cells was observed against autologous Epstein-Barr virus-transformed human B lymphocytes (EBV-B) pretreated with NY-ESO-1 protein and allogeneic NY-ESO-1-expressing melanoma cells (M-1) with compatible HLA class II expression (Figure 3B). The response of CD8 T cells was observed against *NY-ESO-1* mRNA-transfected autologous phytohemagglutinin (PHA)-stimulated CD4 T cells (Figure 3C). The findings indicate that the CD4 and CD8 T cell responses detected by the stimulation with OLPs were directed against naturally processed CD4 and CD8 T cell epitopes, respectively.

Peptide regions recognized by the CD4 and CD8 T cells were investigated using PFA-fixed autologous CD4- and CD8-depleted PBMCs pre-pulsed with individual overlapping peptides in the assays. As shown in Figure 4, peptides 16 (aa 91-108) and 17 (aa 97-114), and peptides 20 (aa 115-132) and 21 (aa 121-138) were the two dominant regions recognized by CD4 T cells. On the other hand, peptides 27 (aa 153-170) and 28 (aa 156-173) made up the dominant region recognized by CD8 T cells.

Restriction molecules involved in the CD4 T cell recognition of peptides 16 (aa 91-108) and 21 (aa 121-138) were investigated. As shown in Figure 5, CD4 T cell recognition of peptides 16 (aa 91-108) and 21 (aa 121-138) was blocked by an anti-DP mAb and an anti-DR mAb, respectively. Analyses using EBV-B cells for which HLA genotypes have been determined showed restriction by DPB1*0501 for the recognition of peptide 16 (aa 91-108) and restriction by DRB1*0101 for the recognition of peptide 21 (aa 121-138).

CD8 T cell recognition of peptide 27 (aa 153-170) was analyzed using tetramers. The sequence SLLMWTQC (aa 157-165) used for preparing A*0206-tetramers lies in peptide 27. As shown in Figure 6B, a significant fraction of A*0206-tetramer positive CD8 T cells were detected in the culture stimulated with OLPs. A*2402-tetramer positive CD8 T cells were at background level.

NY-ESO-1-reactive CD4 and CD8 T cell frequencies

The frequency of CD4 T cells specific for peptides 16 and 21 was determined by limiting dilution. As shown in Figure 6A, the CD4 T cell frequency was calculated as 3.2×10^{-6} with either peptide. The frequency of CD8 T cells positive for A*0206 tetramer staining was 6% (Figure 6B). Multiplication during culture for 12 days, assuming a doubling time of 24 h, was estimated at 1.4×10^{-5}.

Foxp3+ CD25 high T regulatory cells (Tregs) in PBMCs from the patient during the course of the disease

Foxp3+ CD25 high Tregs in PBMCs were examined at three different time points simultaneously by intracellular staining using FACS. As shown in Figure 7, Foxp3+ CD25 high Tregs in normal individuals were in the range of 0% to 2%. In the patient, these cells were detected at frequencies of 1.8% and 4.6% in May 2005 and January 2006, respectively. In March 2009, at the time when obvious tumor progression and a decreased immune response were observed, the number of Foxp3+ CD25 high Tregs went up to 13.4%. Cytokines in the serum were determined by ELISA using specific mAbs. As shown in Figure 8, a gradual increase in TGF-β1 was detected in sera from May 2005 to March 2009. No IL-4 or IL-10 was detected.

Figure 5

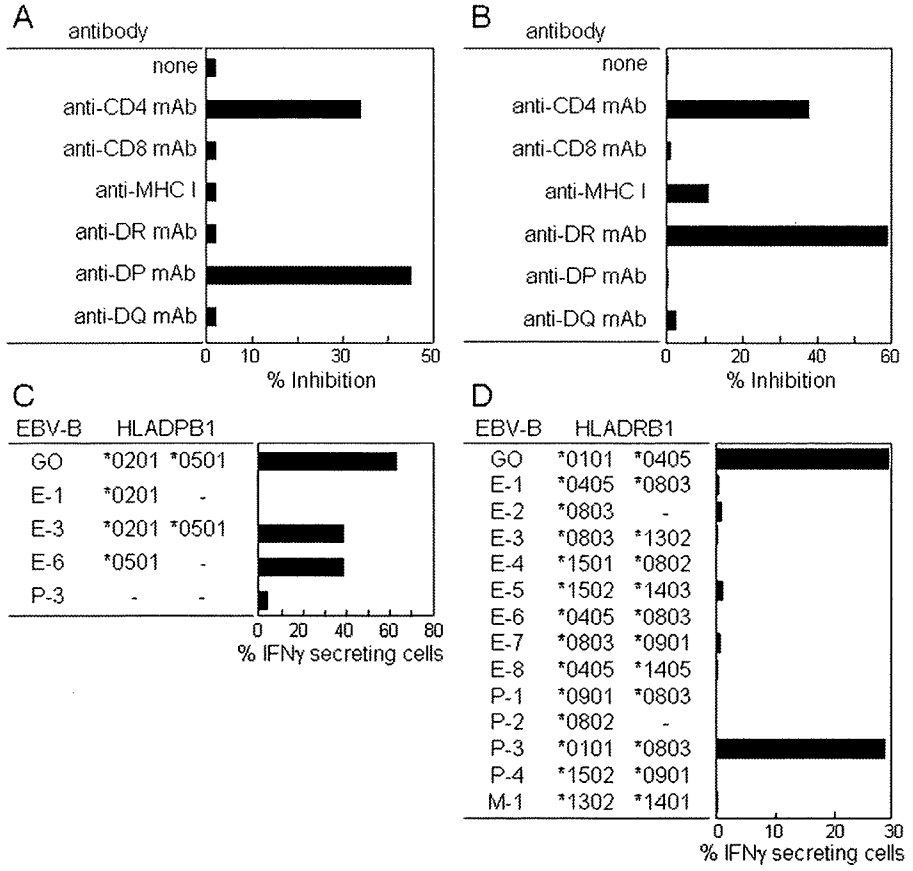

Restriction molecules involved in the CD4 T cell recognition of NY-ESO-1. CD4 T cell recognition of peptide 16 (aa 91-108) (A and C) and peptide 21 (aa 121-138) (B and D) was analyzed by antibody blocking (A and B) and using various EBV-B cells as APCs (C and D). CD4 T cells cultured with irradiated (40 Gy) autologous CD4- and CD8-depleted PBMCs in the presence of a mixture of OLPs for 14 days, as described in the legend of Figure 4, were assayed for IFNγ secretion against PFA-treated autologous CD4- and CD8-depleted PBMCs pre-pulsed with peptide 16 (aa 91-108) (A) and peptide 21 (aa 121-138) (B) in the presence of various mAbs (2 μg/ml) during the assay, and against PFA-treated EBV-B cells as APCs pre-pulsed with peptide 16 (aa 91-108) (1 μg/ml) (C) and peptide 21 (aa 121-138) (1 μg/ml) (D) for which HLA genotypes have been determined. IFNγ production was determined by ELISA in A and B using the supernatant after culture for 18 h and by an IFNγ secretion assay in C and D after stimulation for 4 h.

Discussion

In this study, we show a correlation between a strong NY-ESO-1-specific immune response and its decreasing levels to spontaneous tumor regression of multiple pleural metastases and recurrence, respectively, during the course of the disease in a long-surviving patient with an NY-ESO-1-expressing lung adenocarcinoma. An integrated immune response consisting of IgG antibody and CD4 and CD8 T cells against NY-ESO-1 was observed at the time of spontaneous tumor regression. A tumor mass (3 x 3 cm) in the right hilar lymph node remained the same size for more than a year. After 3 years, a tumor recurred at the primary lesion site, which had disappeared spontaneously before the time of his first visit to the hospital and had been noticed as interstitial thickening on computed tomography. IgG antibody levels and CD4 and CD8 T cells against NY-ESO-1 decreased, but were still detectable. On the other hand, Foxp3+ CD25 high Tregs gradually increased in association with tumor progression. Thus, the decrease in the initially strong immune response against NY-ESO-1 was associated with a gradual increase in Foxp3+ CD25 high Tregs, suggesting a relationship between the NY-ESO-1 immune response and the clinical course of the disease in this lung cancer patient.

Suppression of tumor immune responses by tumors has been well documented in experimental tumors and human cancers (11). Depletion of Tregs in the tumor host by injection of CD25 mAb caused regression in various murine tumors (12). *In vitro* depletion of Tregs from PBMCs in healthy donors and cancer patients unmasked NY-ESO-1 CD4 T cell responses which were otherwise undetectable (13). In human ovarian cancer, the frequency of Tregs in the tumor has been shown to negatively correlate with survival (14) and, in malignant melanoma, a high proportion of Tregs was observed in metastatic tumors (15). We have recently shown a high proportion of Tregs in the blister fluid of local tumor sites in a malignant melanoma patient vaccinated with a complex of cholesterol-bearing hydrophobized pullulan and NY-ESO-1 protein (16). In the peripheral blood, the number of Tregs has also been shown to have increased in various cancers (17). Recently, it was shown that patients with advanced melanoma had a high number of circulating Tregs, and that the number of Tregs in the blood was

Figure 6

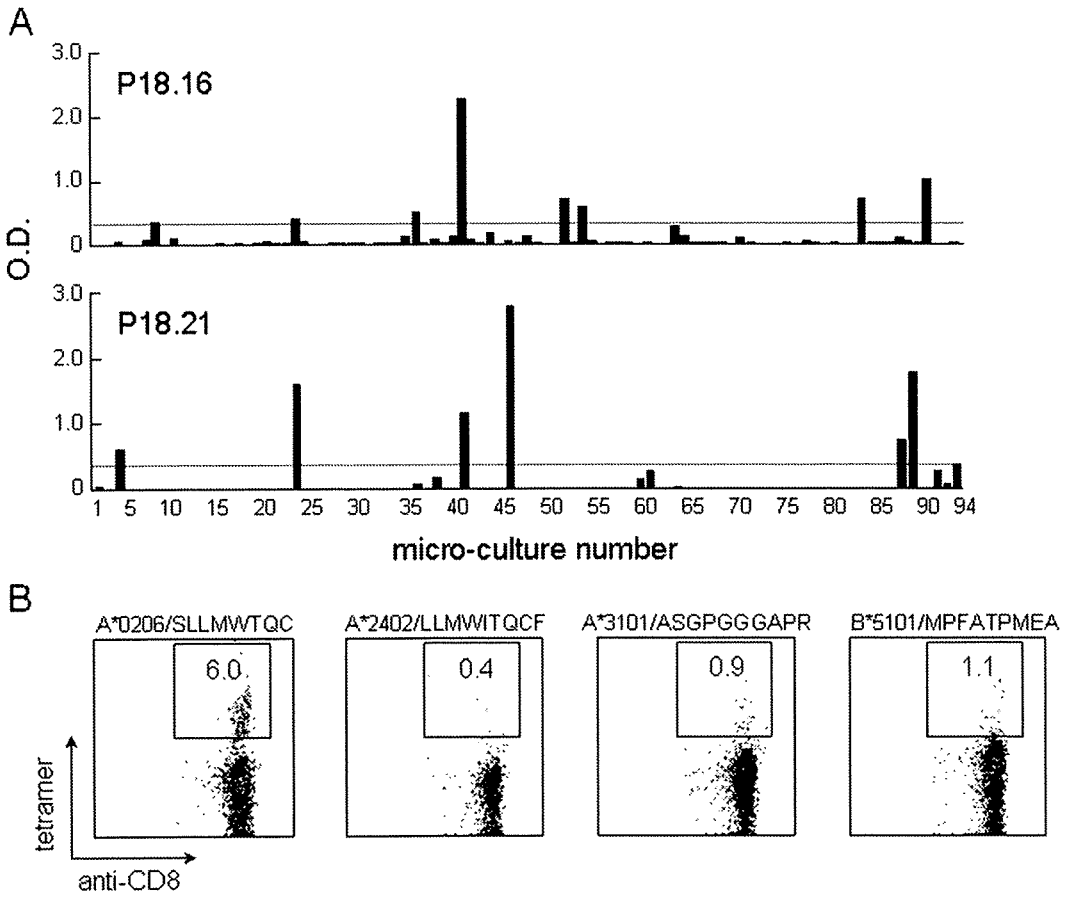

NY-ESO-1-reactive CD4 and CD8 T cell frequencies. Frequency analysis of peptide-specific CD4 T cells (A) and tetramer staining of CD8 T cells (B) are shown. (A) A limited number (2×10^4) of CD4 T cells were seeded in duplicate in 96-well plates and cultured with irradiated (40 Gy) autologous CD4- and CD8-depleted PBMCs (2×10^4) as APCs in the presence of peptides 16 (aa 91-108) (1 μg/ml) (top) and 21 (aa 121-138) (1 μg/ml) (bottom) for 14 days. On the twenty-sixth day after stimulating twice, IFNγ production by the cells in each well was determined against each peptide (1 μg/ml) using autologous EBV-B cells (1×10^4) as APCs by ELISA after incubation for 18 h. An O.D. value exceeding 0.3 after subtraction of the background (without peptide) was taken as positive. The number of positive wells was 6 in both cultures. The peptide-specific CD4 T cell frequency was calculated to be 3.2×10^{-6} for both peptides. (B) Four tetramers were prepared. The patient HLA class I genotype was HLA-A*0206, A*2402, B27, B54, and Cw1. The sequence SLLMWTQC (aa 157-165) used to prepare the A*0206-tetramers lies in peptide 27 (aa 153-170) recognized by the patient's CD8 T cells, as shown in Figure 4.

correlated with the stage of disease and the clinical and immunologic efficacy of the NY-ESO-1 ISCOMATRIX™ cancer vaccine (18).

Immune epitopes of NY-ESO-1 recognized by the IgG antibody and the CD4 and CD8 T cells were determined in the patient. The antibody recognized the amino acid region 1-30 dominantly, and the amino acid regions 81-110 and 151-180 weakly. Recognition of the NY-ESO-1 amino acid region 1-30 is not common in the immune response of Japanese patients with NY-ESO-1-expressing tumors (19). The most common amino acid region recognized by the antibodies corresponds to amino acids 91-108. Eight of 9 patients who had antibodies against NY-ESO-1 responded to the amino acid region 91-108 predominantly (19). Six of 9 patients who were immunized with a complex of cholesterol-hydrophobized pullulan and NY-ESO-1 protein responded to the same region (19). The IgG antibody response to the rather rare epitope region may have been related to the favorable clinical course in this patient. In this regard, we are now trying to produce a human monoclonal antibody using CD19+ B cells from PBMCs of this patient.

Recent analyses of the immune responses of the patients vaccinated with the NY-ESO-1 protein show that most of the CD4 or CD8 T cell responses were directed against two dominant regions in the NY-ESO-1 molecule (20-23). One was the region corresponding to aa 73-114 and the other corresponds to aa 115-144 (22). In this study, we determined that the two epitope regions recognized by CD4 T cells lie in the two previously described dominant regions and that the epitope region recognized by CD8 T cells is in the C-terminus. One of the epitopes recognized by the CD4 T cells was peptide 91-114, for which recognition was restricted to DPB1*0501. This peptide is in a region frequently recognized by the antibody (as described above) and also by CD4 and CD8 T cells, for which restriction molecules have not been fully elucidated. The other was peptide 115-138, for which recognition was restricted to DRB1*0101. Zarour *et al.* (24) originally identified the peptide 119-143 as a promiscuous HLA class II epitope that binds to

Figure 7

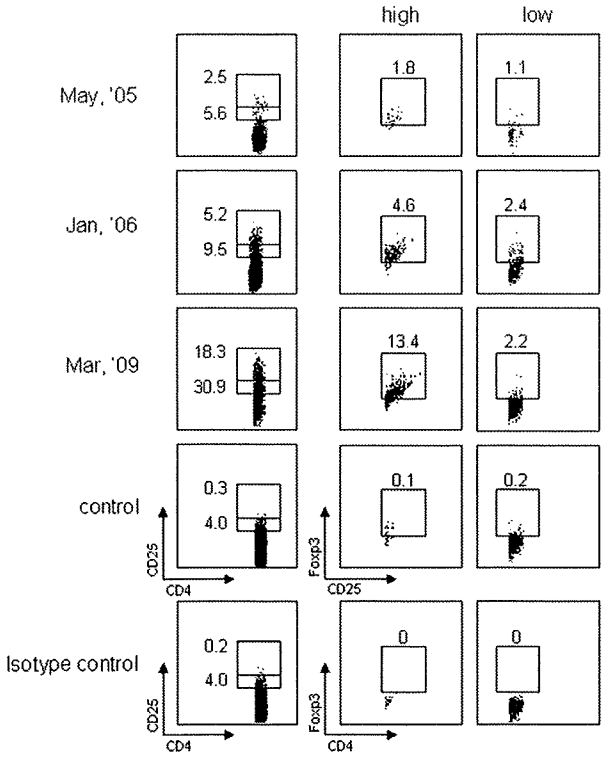

Flow cytometry of Foxp3+ CD25+ CD4 T regulatory cells at different time points. CD25 high and low CD4 T cells were analyzed for Foxp3 expression by intracellular staining using FACS Calibur. A normal individual was used as control.

multiple DR molecules such as DRB1*0101, DRB1*0401, DRB1*0701, DRB1*1101, DRB1*1501, DRB3*0101, DRB4*0101 and DRB5*0101 expressed at a high frequency in Caucasian populations. Recently, the shorter peptide 122-138 was shown to bind to DRB1*0802, DRB1*0901, DRB1*1502, and DRB1*0405/*0410, which are common DR alleles in the Japanese population (25). The promiscuous peptide 119-143 was also shown to contain multiple HLA class I epitopes that bound to A66, A68, Cw3 and Cw15 (26). The epitope recognized by CD8 T cells in the patient was restricted to *A0206, as demonstrated by tetramer staining. The peptide epitope 157-165 was identified as the immunodominant *A0201 epitope and was also shown to bind to *A0206 (27). The strong immunogenicity of these peptide epitopes may have contributed to the rather high frequency of NY-ESO-1-specific CD4 and CD8 T cells in this patient.

Abbreviations

OLPs, overlapping peptides; PFA, paraformaldehyde

Acknowledgements

We thank Ms. K. Nishida for tetramer production and Ms. J. Mizuuchi for preparation of the manuscript. We also thank Dr. L. J. Old for continuous encouragement during this study. This work was supported in part by a Grant-in-Aid for Scientific Research on Priority Areas from the Ministry of Education, Culture, Sports, Science and Technology of Japan.

Figure 8

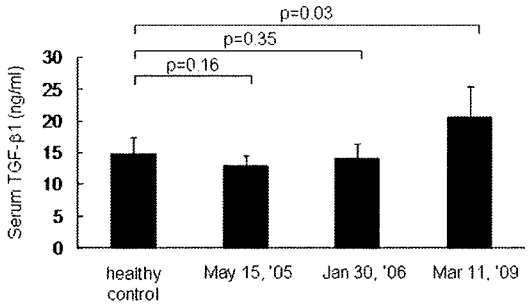

Serum TGF-β1 determined by ELISA.

References

1. Chen YT, Scanlan MJ, Sahin U, Türeci O, Güre AO, Tsang S, Williamson B, Stockert E, Pfreundschuh M, Old LJ. A testicular antigen aberrantly expressed in human cancers detected by autologous antibody screening. *Proc Natl Acad Sci USA* 1997; **94:** 1914-1918. (PMID: 9050879)

2. Scanlan MJ, Güre AO, Jungbluth AA, Old LJ, Chen YT. Cancer/testis antigens: an expanding family of targets for cancer immunotherapy. *Immunol Rev* 2002; **188:** 22-32. (PMID: 12445278)

3. Simpson AJ, Caballero OL, Jungbluth A, Chen YT, Old LJ. Cancer/testis antigens, gametogenesis and cancer. *Nat Rev Cancer* 2005; **5:** 615-625. (PMID: 16034368)

4. Jungbluth AA, Chen YT, Stockert E, Busam KJ, Kolb D, Iversen K, Coplan K, Williamson B, Altorki N, Old LJ. Immunohistochemical analysis of NY-ESO-1 antigen expression in normal and malignant human tissues. *Int J Cancer* 2001; **92:** 856-860. (PMID: 11351307)

5. Gnjatic S, Nishikawa H, Jungbluth AA, Güre AO, Ritter G, Jäger E, Knuth A, Chen YT, Old LJ. NY-ESO-1: Review of an immunogenic tumor antigen. *Adv Cancer Res* 2006; **95:** 1-30. (PMID: 16860654)

6. Stockert E, Jäger E, Chen YT, Scanlan MJ, Gout I, Karbach J, Arand M, Knuth A, Old LJ. A survey of the humoral immune response of cancer patients to a panel of human tumor antigens. *J Exp Med* 1998; **187:** 1349-1354. (PMID: 9547346)

7. Jäger E, Stockert E, Zidianakis Z, Chen YT, Karbach J, Jäger D, Arand M, Ritter G, Old LJ, Knuth A. Humoral immune responses of cancer patients against "Cancer-Testis" antigen NY-ESO-1: correlation with clinical events. *Int J Cancer* 1999; **84:** 506-510. (PMID: 10502728)

8. Gnjatic S, Atanackovic D, Jäger E, Matsuo M, Selvakumar A, Altorki NK, Maki RG, Dupont B, Ritter G, Chen YT, Knuth A, Old LJ. Survey of naturally occurring CD4+ T cell responses against NY-ESO-1 in cancer patients: correlation with antibody responses. *Proc Natl Acad Sci USA* 2003; **100:** 8862-8867. (PMID: 12853579)

9. Jäger E, Nagata Y, Gnjatic S, Wada H, Stockert E, Karbach J, Dunbar PR, Lee SY, Jungbluth A, Jäger D, Arand M, Ritter G, Cerundolo V, Dupont B, Chen YT, Old LJ, Knuth A. Monitoring CD8 T cell

responses to NY-ESO-1: correlation of humoral and cellular immune responses. *Proc Natl Acad Sci USA* 2000; **97:** 4760-4765. (PMID: 10781081)

10. Nakamura Y, Noguchi Y, Sato E, Uenaka A, Sato S, Kitazaki T, Kanda T, Soda H, Nakayama E, Kohno S. Spontaneous remission of a non-small cell lung cancer possibly caused by anti-NY-ESO-1 immunity. *Lung Cancer* 2009; **65:** 119-122. (PMID: 19193472)

11. Zou W. Immunosuppressive networks in the tumour environment and their therapeutic relevance. *Nat Rev Cancer* 2005; **5:** 263-274. (PMID: 15776005)

12. Onizuka S, Tawara I, Shimizu J, Sakaguchi S, Fujita T, Nakayama E. Tumor rejection by in vivo administration of anti-CD25 (interleukin-2 receptor alpha) monoclonal antibody. *Cancer Res* 1999; **59:** 3128-3133. (PMID: 10397255)

13. Nishikawa H, Jäger E, Ritter G, Old LJ, Gnjatic S. CD4+ CD25+ regulatory T cells control the induction of antigen-specific CD4+ helper T cell responses in cancer patients. *Blood* 2005; **106:** 1008-1011. (PMID: 15840697)

14. Sato E, Olson SH, Ahn J, Bundy B, Nishikawa H, Qian F, Jungbluth AA, Frosina D, Gnjatic S, Ambrosone C, Kepner J, Odunsi T, Ritter G, Lele S, Chen YT, Ohtani H, Old LJ, Odunsi K. Intraepithelial CD8+ tumor-infiltrating lymphocytes and a high CD8+/regulatory T cell ratio are associated with favorable prognosis in ovarian cancer. *Proc Natl Acad Sci USA* 2005; **102:** 18538-18543. (PMID: 16344461)

15. Méndez R, Ruiz-Cabello F, Rodríguez T, Del Campo A, Paschen A, Schadendorf D, Garrido F. Identification of different tumor escape mechanisms in several metastases from a melanoma patient undergoing immunotherapy. *Cancer Immunol Immunother* 2007; **56:** 88-94. (PMID: 16622680)

16. Tsuji K, Hamada T, Uenaka A, Wada H, Sato E, Isobe M, Asagoe K, Yamasaki O, Shiku H, Ritter G, Murphy R, Hoffman EW, Old LJ, Nakayama E, Iwatsuki K. Induction of immune response against NY-ESO-1 by CHP-NY-ESO-1 vaccination and immune regulation in a melanoma patient. *Cancer Immunol Immunother* 2008; **57:** 1429-1437. (PMID: 18311489)

17. Beyer M, Schultze JL. Regulatory T cells in cancer. *Blood* 2006; **108:** 804-811. (PMID: 16861339)

18. Nicholaou T, Ebert LM, Davis ID, McArthur GA, Jackson H, Dimopoulos N, Tan B, Maraskovsky E, Miloradovic L, Hopkins W, Pan L, Venhaus R, Hoffman EW, Chen W, Cebon J. Regulatory T-cell-mediated attenuation of T-cell responses to the NY-ESO-1 ISCOMATRIX vaccine in patients with advanced malignant melanoma. *Clin Cancer Res* 2009; **15:** 2166-2173. (PMID: 19276262)

19. Kawabata R, Wada H, Isobe M, Saika T, Sato S, Uenaka A, Miyata H, Yasuda T, Doki Y, Noguchi Y, Kumon H, Tsuji K, Iwatsuki K, Shiku H, Ritter G, Murphy R, Hoffman E, Old LJ, Monden M, Nakayama E. Antibody response against NY-ESO-1 in CHP-NY-ESO-1 vaccinated patients. *Int J Cancer* 2007; **120:** 2178-2184. (PMID: 17278093)

20. Davis ID, Chen W, Jackson H, Parente P, Shackleton M, Hopkins W, Chen Q, Dimopoulos N, Luke T, Murphy R, Scott AM, Maraskovsky E, McArthur G, MacGregor D, Sturrock S, Tai TY, Green S, Cuthbertson A, Maher D, Miloradovic L, Mitchell SV, Ritter G, Jungbluth AA, Chen YT, Gnjatic S, Hoffman EW, Old LJ, Cebon JS. Recombinant NY-ESO-1 protein with ISCOMATRIX adjuvant induces broad integrated antibody and CD4(+) and CD8(+) T cell responses in humans. *Proc Natl Acad Sci USA* 2004; **101:** 10697-10702. (PMID: 15252201)

21. Jäger E, Karbach J, Gnjatic S, Neumann A, Bender A, Valmori D, Ayyoub M, Ritter E, Ritter G, Jäger D, Panicali D, Hoffman E, Pan L, Oettgen H, Old LJ, Knuth A. Recombinant vaccinia/fowlpox NY-ESO-1 vaccines induce both humoral and cellular NY-ESO-1-specific immune responses in cancer patients. *Proc Natl Acad Sci USA* 2006; **103:** 14453-14458. (PMID: 16984998)

22. Uenaka A, Wada H, Isobe M, Saika T, Tsuji K, Sato E, Sato S, Noguchi Y, Kawabata R, Yasuda T, Doki Y, Kumon H, Iwatsuki K, Shiku H, Monden M, Jungbluth AA, Ritter G, Murphy R, Hoffman E, Old LJ, Nakayama E. T cell immunomonitoring and tumor responses in patients immunized with a complex of cholesterol-bearing hydrophobized pullulan (CHP) and NY-ESO-1 protein. *Cancer Immun* 2007; **7:** 9. URL: http://www.cancerimmunity.org/v7p9/070309.htm

23. Valmori D, Souleimanian NE, Tosello V, Bhardwaj N, Adams S, O'Neill D, Pavlick A, Escalon JB, Cruz CM, Angiulli A, Angiulli F, Mears G, Vogel SM, Pan L, Jungbluth AA, Hoffmann EW, Venhaus R, Ritter G, Old LJ, Ayyoub M. Vaccination with NY-ESO-1 protein and CpG in Montanide induces integrated antibody/Th1 responses and CD8 T cells through cross-priming. *Proc Natl Acad Sci USA* 2007; **104:** 8947-8952. (PMID: 17517626)

24. Zarour HM, Maillere B, Brusic V, Coval K, Williams E, Pouvelle-Moratille S, Castelli F, Land S, Bennouna J, Logan T, Kirkwood JM. NY-ESO-1 119-143 is a promiscuous major histocompatibility complex class II T-helper epitope recognized by Th1- and Th2-type tumor-reactive CD4+ T cells. *Cancer Res* 2002; **62:** 213-218. (PMID: 11782380)

25. Ohkuri T, Sato M, Abe H, Tsuji K, Yamagishi Y, Ikeda H, Matsubara N, Kitamura H, Nishimura T. Identification of a novel NY-ESO-1 promiscuous helper epitope presented by multiple MHC class II molecules found frequently in the Japanese population. *Cancer Sci* 2007; **98:** 1092-1098. (PMID: 17488334)

26. Matsuzaki J, Qian F, Luescher I, Lele S, Ritter G, Shrikant PA, Gnjatic S, Old LJ, Odunsi K. Recognition of naturally processed and ovarian cancer reactive CD8+ T cell epitopes within a promiscuous HLA class II T-helper region of NY-ESO-1. *Cancer Immunol Immunother* 2008; **57:** 1185-1195. (PMID: 18253733)

27. Chen WF. Identification and characterization of human hepatocellular carcinoma-associated antigens [abstract]. *Cancer Immun* 2005; **5 Suppl 1:** 21. URL: http://www.cancerimmunity.org/v5suppl1p21/041242_abs.htm

28. Uenaka A, Ono T, Akisawa T, Wada H, Yasuda T, Nakayama E. Identification of a unique antigen peptide pRL1 on BALB/c RL male 1 leukemia recognized by cytotoxic T lymphocytes and its relation to the Akt oncogene. *J Exp Med* 1994; **180:** 1599-1607. (PMID: 7964448)

29. Altman JD, Moss PA, Goulder PJ, Barouch DH, McHeyzer-Williams MG, Bell JI, McMichael AJ, Davis MM. Phenotypic analysis of antigen-specific T lymphocytes. *Science* 1996; **274:** 94-96. (PMID: 8810254)

30. Morishima S, Akatsuka Y, Nawa A, Kondo E, Kiyono T, Torikai H, Nakanishi T, Ito Y, Tsujimura K, Iwata K, Ito K, Kodera Y, Morishima Y, Kuzushima K, Takahashi T. Identification of an HLA-A24-restricted cytotoxic T lymphocyte epitope from human papillomavirus type-16 E6: the combined effects of bortezomib and interferon-gamma on the presentation of a cryptic epitope. *Int J Cancer* 2007; **120:** 594-604. (PMID: 17096336)

31. Yamaguchi H, Tanaka F, Ohta M, Inoue H, Mori M. Identification of HLA-A24-restricted CTL epitope from cancer-testis antigen, NY-ESO-1, and induction of a specific antitumor immune response. *Clin Cancer Res* 2004; **10:** 890-896. (PMID: 14871964)

32. Wang RF, Johnston SL, Zeng G, Topalian SL, Schwartzentruber DJ, Rosenberg SA. A breast and melanoma-shared tumor antigen: T cell responses to antigenic peptides translated from different open reading frames. *J Immunol* 1998; **161:** 3598-3606. (PMID: 9759882)

33. Jäger E, Karbach J, Gnjatic S, Jäger D, Maeurer M, Atmaca A, Arand M, Skipper J, Stokert E, Chen YT, Old LJ, Knuth A. Identification of a naturally processed NY-ESO-1 peptide recognized by CD8+ T cells in the context of HLA-B51. *Cancer Immun* 2002; **2:** 12. URL: http://www.cancerimmunity.org/v2p12/020812.htm

34. Tsukahara T, Kawaguchi S, Torigoe T, Asanuma H, Nakazawa E, Shimozawa K, Nabeta Y, Kimura S, Kaya M, Nagoya S, Wada T, Yamashita T, Sato N. Prognostic significance of HLA class I expression in osteosarcoma defined by anti-pan HLA class I monoclonal antibody, EMR8-5. *Cancer Sci* 2006; **97:** 1374-1380. (PMID: 16995877)

Materials and methods

Patient clinical course

Patient GO is a 71-year-old Japanese man with a lung adenocarcinoma. His clinical course from November 2004 to September 2007 was reported previously (10). Briefly, in November 2004, a right hilar mass and multiple pleural dissemination of the tumor were found. Pathological diagnosis based on specimens of the pleural tumors was poorly differentiated adenocarcinoma. Surprisingly, by March 2005, the pleural dissemination disappeared without any treatment. In February 2006, the right hilar mass increased in size. In November 2007, a new lesion appeared in the right lower lobe which was noticed as interstitial thickening by chest computed tomography. It appeared to be a recurrence of the primary tumor which had disappeared before his first visit to the hospital. Chemotherapy (carboplatin and gemcitabine, 4 cycles) was started in November 2007, but the tumor gradually increased in size and pleural effusion appeared. Second line chemotherapy (gemcitabine, 2 cycles) was started in March 2009. No other metastatic lesion was observed as of April 2009.

Blood samples

Peripheral blood was drawn from the patient with informed consent. Peripheral blood mononuclear cells (PBMCs) and plasma were isolated by density gradient centrifugation using Histo-Paque 1077 (Sigma-Aldrich, St. Louis, MO). CD4 and CD8 T cells were purified from PBMCs using CD4 and CD8 microbeads, respectively, with a large scale column and a magnetic device (Miltenyi Biotec, Auburn, CA). The residual cells were used as CD4- and CD8-depleted cells. The cells were stored in liquid N_2 until use. HLA typing of PBMCs was done using a sequence-specific oligonucleotide probe and sequence-specific priming of genomic DNA using standard procedures.

Cell lines

EBV-B cells were generated from CD19+ peripheral blood B cells using the culture supernatant from the EBV-producing B95-8 cells. A melanoma cell line M-1 was established from the surgically resected primary tumor.

Peptides

The following series of 28 overlapping 18-mer peptides spanning the NY-ESO-1 protein were synthesized: 18.1 (1-18), 18.2 (7-24), 18.3 (13-30), 18.4 (19-36), 18.5 (25-42), 18.6 (31-48), 18.7 (37-54), 18.8 (43-60), 18.9 (49-66), 18.10 (55-72), 18.11 (61-78), 18.12 (67-84), 18.13 (73-90), 18.14 (79-96), 18.15 (85-102), 18.16 (91-108), 18.17 (97-114), 18.18 (103-120), 18.19 (109-126), 18.20 (115-132), 18.21 (121-138), 18.22 (127-144), 18.23 (133-150), 18.24 (139-156), 18.25 (145-162), 18.26 (149-166), 18.27 (153-170) and 18.28 (156-173). Nine 30-mer peptides spanning the protein were also synthesized: 30.1 (1-30), 30.2 (21-50), 30.3 (41-70), 30.4 (61-90), 30.5 (81-110), 30.6 (101-130), 30.7 (121-150), 30.8 (141-170) and 30.9 (151-180). These peptides were synthesized using standard solid-phase methods based on N-(9-fluorenyl)-methoxycarbonyl (Fmoc) chemistry on an ABIMED Multiple Peptide Synthesizer (AMS422, ABIMED, Langenfeld, Germany) at Okayama University (Okayama, Japan).

Recombinant proteins

Recombinant NY-ESO-1 (1) and RL-Akt (28) proteins were prepared as described previously. cDNAs for NY-ESO-1 and RL-Akt were cloned into the *Sph*I/*Sal*I and *Bam*HI/*Sph*I sites of the pQE-30 vector. N-His tagged protein was purified by nickel-ion affinity chromatography under denaturing conditions.

Preparation of mRNA

The NY-ESO-1 plasmid was linearized with the restriction enzyme *Nde*I, transcribed *in vitro* using T7 polymerase (mMESSAGE mMACHINE™ T7 Kit, Ambion, Austin, TX) and polyadenylated using poly (A) polymerase [Poly (A) Tailing kit, Ambion] according to the manufacturer's instructions. The capped and tailed RNA was resuspended in water and stored at -80°C before use.

Electroporation of mRNA

The cells (approx. 5 x 10^6) in X-VIVO 20 medium (100 µl) and mRNA (20 µg) were mixed and transferred to a 2-mm gap cuvette (BTX Genetronics, San Diego, CA) and electroporated using a BTX 830 square wave electroporator. The cells were immediately suspended in X-VIVO 20 medium (2 ml) and cultured for 18 h to 24 h in 24-well plates at 37°C in a 5% CO_2 atmosphere.

Antibody ELISA

Antibody responses to NY-ESO-1 protein or synthetic peptides were evaluated by enzyme-linked immunosorbent assay (ELISA) as described elsewhere (19). Recombinant protein (1 µg/ml) or peptide (5 µg/ml) in a coating buffer (15 mM Na_2CO_3, 30 mM $NaHCO_3$, pH 9.6) was adsorbed onto 96-well Polysorp immunoplates (Nunc, Roskilde, Denmark) and incubated overnight at 4°C. Plates were washed with PBS and blocked with 200 µl/well of 5% FCS/PBS for 1 h at room temperature. After washing, 100 µl of serially diluted serum was added to each well and the plates incubated for 2 h at room

temperature. After extensive washing, goat anti-human IgG (Medical & Biological Laboratories, Nagoya, Japan) or mouse anti-human IgM, IgG1, IgG2, IgG3 or IgG4-HRP (Southern Biotechnologies, Birmingham, AL) was added to the wells as a second antibody, and the plates were incubated for 1 h at room temperature. After washing, signals were developed with 100 µl per well of 0.03% o-phenylene diamine dihydrochloride (OPDA, Wako, Osaka, Japan), 0.02% hydrogen peroxide and 0.15 M citrate buffer, and the absorbance at 490 nm was read using an ELISA reader (Benchmark Microplate Reader; Bio-Rad, Hercules, CA). Recombinant RL-Akt (28) was used as control protein.

IFNγ ELISA

CD4 T cells (1×10^4) and paraformaldehyde (PFA) (0.2%)-treated EBV-B cells (1×10^4) pre-pulsed with the peptides or pretreated with the protein were cultured in a 96-well round-bottomed culture plate at 37°C in a 5% CO_2 atmosphere. After 18 h, culture supernatants were collected and the amount of IFNγ was measured by sandwich ELISA.

TGF-β1 ELISA

Serum TGF-β1 was estimated by DuoSet Sandwich ELISA (R&D Systems, Minneapolis, MN) according to the manufacturer's instructions. The serum was treated with activation reagent for 10 min at room temperature, followed by addition of a neutralization reagent. Treated samples were transferred to ELISA plates coated with a capture antibody. Recombinant human TGF-β1 was used as a standard.

In vitro stimulation of CD4 and CD8 T cells

Frozen cells were thawed and resuspended in AIM-V medium (Invitrogen, Carlsbad, CA) supplemented with 5% heat-inactivated pooled human serum (CM), and kept at 37°C in a 5% CO_2 atmosphere for 2 h. CD4 and CD8 T cells (2×10^6) were cultured with irradiated (40 Gy) autologous CD4- and CD8-depleted PBMCs (2×10^6) as antigen-presenting cells (APCs) in the presence of 28 overlapping 18-mer peptides and a 30-mer C-terminal peptide (OLPs) spanning the entire NY-ESO-1 protein (1 µg /ml for each peptide) in 2 ml of CM supplemented with 10 units/ml rIL-2 (Takeda Chemical Industries, Osaka, Japan) and 10 ng/ml rIL-7 (Peprotech, London, UK) in a 24-well culture plate at 37°C in a 5% CO_2 atmosphere for 12 days. For the second stimulation, 1×10^6 instead of 2×10^6 responder cells were used in the culture described above.

IFNγ secretion assay

Responder CD4 or CD8 T cells (1×10^5) were stimulated with paraformaldehyde (PFA) (0.2%)-treated autologous EBV-B cells (1×10^5) pre-pulsed with the peptides for 30 min. The cells were then washed and suspended in 100 µl of RPMI medium, and treated with bi-specific CD45 and IFNγ antibody (IFNγ catch reagent) (2 µl) for 5 min on ice. The cells were then diluted in AIM-V medium (1 ml) and placed on a slow rotating device (Miltenyi Biotec) to allow IFNγ secretion at 37°C in a 5% CO_2 atmosphere. After incubation for 50 min, the cells were washed with cold buffer and treated with PE-conjugated anti-IFNγ (detection reagent), and FITC-conjugated anti-CD4 or anti-CD8 mAb. After incubation for 10 min at 4°C, the cells were washed and analyzed with a FACS Calibur (Becton Dickinson).

Tetramer construction and staining

HLA-peptide tetramers were produced as described previously (29, 30). A*0206 (27), A24 (31), A31 (32) and B51 (33) tetramers were used. For staining, cells were incubated with tetramer at a concentration of 20 µg/ml for 15 min at room temperature, followed by incubation with FITC-conjugated anti-CD8 mAb (Miltenyi Biotec) on ice for 15 min and analyzed with a FACS Calibur (Becton Dickinson).

Intracellular Foxp3 staining

Triple staining was carried out using monoclonal antibodies (mAb). Staining with CD4 mAb (eBioscience, San Diego, CA) and CD25 mAb (Becton Dickinson) was performed according to the manufacturer's instructions. Intracellular Foxp3 staining using clone PC101 (eBioscience) was carried out using the Foxp3 Staining Buffer Set (eBioscience). The analysis was carried out on a FACS Calibur (Becton Dickinson).

Immunohistochemistry (IHC)

IHC was performed as described (4). E978 (4) and EMR8-5 (Funakoshi, Tokyo, Japan) (34) mAbs were used for the analysis of NY-ESO-1 and HLA class I expression, respectively.

Contact

Address correspondence to:

Eiichi Nakayama, M.D.
Department of Immunology
Okayama University Graduate School of Medicine, Dentistry and Pharmaceutical Sciences
2-5-1 Shikata-cho
Kita-ku, Okayama 700-8558
Japan
Tel.: + 81 86 235-7187
Fax: + 81 86 235-7193
E-mail: nakayama@md.okayama-u.ac.jp

Vol 459|4 June 2009|doi:10.1038/nature07969

LETTERS

Frequent inactivation of A20 in B-cell lymphomas

Motohiro Kato[1,2], Masashi Sanada[1,5], Itaru Kato[6], Yasuharu Sato[7], Junko Takita[1,2,3], Kengo Takeuchi[8], Akira Niwa[6], Yuyan Chen[1,2], Kumi Nakazaki[1,4,5], Junko Nomoto[9], Yoshitaka Asakura[9], Satsuki Muto[1], Azusa Tamura[1], Mitsuru Iio[1], Yoshiki Akatsuka[11], Yasuhide Hayashi[12], Hiraku Mori[13], Takashi Igarashi[2], Mineo Kurokawa[4], Shigeru Chiba[3], Shigeo Mori[14], Yuichi Ishikawa[8], Koji Okamoto[10], Kensei Tobinai[9], Hitoshi Nakagama[10], Tatsutoshi Nakahata[6], Tadashi Yoshino[7], Yukio Kobayashi[9] & Seishi Ogawa[1,5]

A20 is a negative regulator of the NF-κB pathway and was initially identified as being rapidly induced after tumour-necrosis factor-α stimulation[1]. It has a pivotal role in regulation of the immune response and prevents excessive activation of NF-κB in response to a variety of external stimuli[2–7]; recent genetic studies have disclosed putative associations of polymorphic *A20* (also called *TNFAIP3*) alleles with autoimmune disease risk[8,9]. However, the involvement of A20 in the development of human cancers is unknown. Here we show, using a genome-wide analysis of genetic lesions in 238 B-cell lymphomas, that *A20* is a common genetic target in B-lineage lymphomas. A20 is frequently inactivated by somatic mutations and/or deletions in mucosa-associated tissue lymphoma (18 out of 87; 21.8%) and Hodgkin's lymphoma of nodular sclerosis histology (5 out of 15; 33.3%), and, to a lesser extent, in other B-lineage lymphomas. When re-expressed in a lymphoma-derived cell line with no functional *A20* alleles, wild-type A20, but not mutant A20, resulted in suppression of cell growth and induction of apoptosis, accompanied by downregulation of NF-κB activation. The A20-deficient cells stably generated tumours in immunodeficient mice, whereas the tumorigenicity was effectively suppressed by re-expression of A20. In A20-deficient cells, suppression of both cell growth and NF-κB activity due to re-expression of A20 depended, at least partly, on cell-surface-receptor signalling, including the tumour-necrosis factor receptor. Considering the physiological function of A20 in the negative modulation of NF-κB activation induced by multiple upstream stimuli, our findings indicate that uncontrolled signalling of NF-κB caused by loss of A20 function is involved in the pathogenesis of subsets of B-lineage lymphomas.

Malignant lymphomas of B-cell lineages are mature lymphoid neoplasms that arise from various lymphoid tissues[10,11]. To obtain a comprehensive registry of genetic lesions in B-lineage lymphomas, we performed a single nucleotide polymorphism (SNP) array analysis of 238 primary B-cell lymphoma specimens of different histologies, including 64 samples of diffuse large B-cell lymphomas (DLBCLs), 52 follicular lymphomas, 35 mantle cell lymphomas (MCLs), and 87 mucosa-associated tissue (MALT) lymphomas (Supplementary Table 1). Three Hodgkin's-lymphoma-derived cell lines were also analysed. Interrogating more than 250,000 SNP sites, this platform permitted the identification of copy number changes at an average resolution of less than 12 kilobases (kb). The use of large numbers of SNP-specific probes is a unique feature of this platform, and combined with the CNAG/AsCNAR software, enabled accurate determination of 'allele-specific' copy numbers, and thus allowed for sensitive detection of loss of heterozygosity (LOH) even without apparent copy-number reduction, in the presence of up to 70–80% normal cell contamination[12,13].

Lymphoma genomes underwent a wide range of genetic changes, including numerical chromosomal abnormalities and segmental gains and losses of chromosomal material (Supplementary Fig. 1), as well as copy-number-neutral LOH, or uniparental disomy (Supplementary Fig. 2). Each histology type had a unique genomic signature, indicating a distinctive underlying molecular pathogenesis for different histology types (Fig. 1a and Supplementary Fig. 3). On the basis of the genomic signatures, the initial pathological diagnosis of MCL was re-evaluated and corrected to DLBCL in two cases. Although most copy number changes involved large chromosomal segments, a number of regions showed focal gains and deletions, accelerating identification of their candidate gene targets. After excluding known copy number variations, we identified 46 loci showing focal gains (19 loci) or deletions (27 loci) (Supplementary Tables 2 and 3 and Supplementary Fig. 4).

Genetic lesions on the NF-κB pathway were common in B-cell lymphomas and found in approximately 40% of the cases (Supplementary Table 1), underpinning the importance of aberrant NF-κB activation in lymphomagenesis[11,14] in a genome-wide fashion. They included focal gain/amplification at the *REL* locus (16.4%) (Fig. 1b) and *TRAF6* locus (5.9%), as well as focal deletions at the *PTEN* locus (5.5%) (Supplementary Figs 1 and 4). However, the most striking finding was the common deletion at 6q23.3 involving a 143-kb segment. It exclusively contained the *A20* gene (also called *TNFAIP3*), a negative regulator of NF-κB activation[3–7,15] (Fig. 1b), which was previously reported as a candidate target of 6q23 deletions in ocular lymphoma[16]. LOH involving the *A20* locus was found in 50 cases, of which 12 showed homozygous deletions as determined by the loss of both alleles in an allele-specific copy number analysis (Fig. 1b, Table 1 and Supplementary Table 4). On the basis of this finding, we searched for possible tumour-specific mutations of *A20* by genomic DNA sequencing of entire coding exons of the gene in the same series of lymphoma samples (Supplementary Fig. 5). Because two out of the three Hodgkin's-lymphoma-derived cell lines had biallelic *A20* deletions/mutations (Supplementary Fig. 6), 24 primary samples from Hodgkin's lymphoma were also analysed for mutations, where

[1]Cancer Genomics Project, Department of [2]Pediatrics, [3]Cell Therapy and Transplantation Medicine, and [4]Hematology and Oncology, Graduate School of Medicine, University of Tokyo, 7-3-1 Hongo, Bunkyo-ku, Tokyo 113-8655, Japan. [5]Core Research for Evolutional Science and Technology, Japan Science and Technology Agency, 4-1-8, Honcho, Kawaguchi-shi, Saitama 332-0012, Japan. [6]Department of Pediatrics, Graduate School of Medicine, Kyoto University, 54 Kawahara-cho, Shogoin, Sakyo-ku, Kyoto 606-8507, Japan. [7]Department of Pathology, Okayama University Graduate School of Medicine, Dentistry and Pharmaceutical Sciences, 2-5-1 Shikata-cho, Kita-ku, Okayama 700-8558, Japan. [8]Division of Pathology, The Cancer Institute of Japanese Foundation for Cancer Research, Japan, 3-10-6 Ariake, Koto-ku, Tokyo 135-8550, Japan. [9]Hematology Division, Hospital, and [10]Early Oncogenesis Research Project, Research Institute, National Cancer Center, 5-1-1 Tsukiji, Chuo-ku, Tokyo 104-0045, Japan. [11]Division of Immunology, Aichi Cancer Center Research Institute, 1-1 Kanokoden, Chikusa-ku, Nagoya 464-8681, Japan. [12]Gunma Children's Medical Center, 779 Shimohakoda, Hokkitsu-machi, Shibukawa 377-8577, Japan. [13]Division of Hematology, Internal Medicine, Showa University Fujigaoka Hospital, 1-30, Fujigaoka, Aoba-ku, Yokohama-shi, Kanagawa 227-8501, Japan. [14]Department of Pathology, Teikyo University School of Medicine, 2-11-1 Kaga, Itabashi-ku, Tokyo 173-8605, Japan.

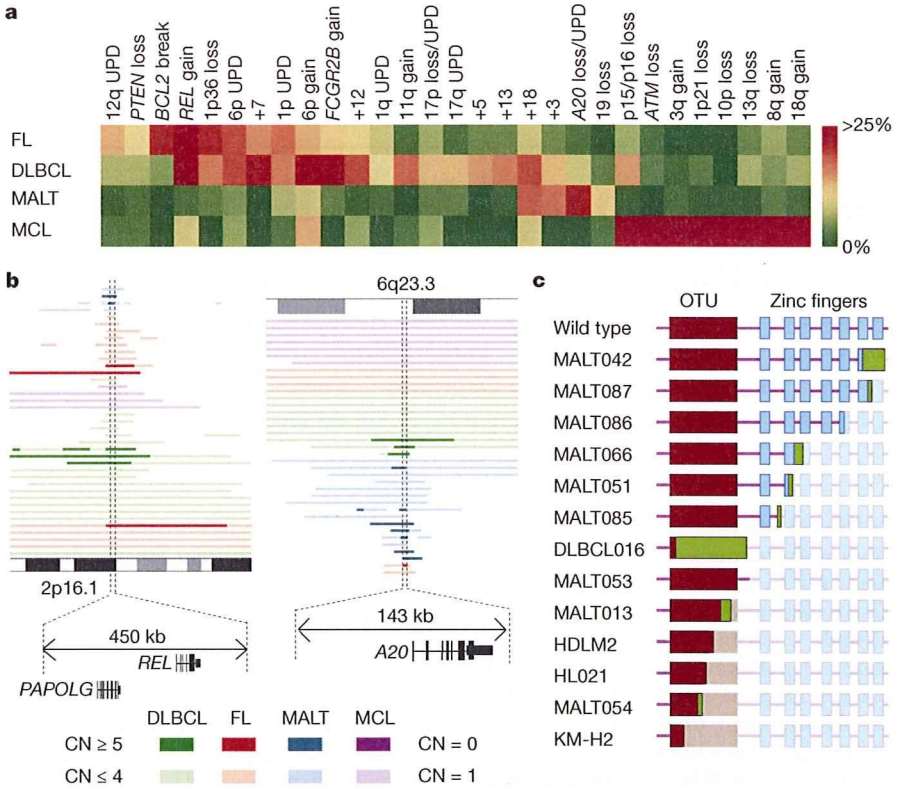

Figure 1 | Genomic signatures of different B-cell lymphomas and common genetic lesions at 2p16-15 and 6q23.3 involving NF-κB pathway genes. **a**, Twenty-nine genetic lesions were found in more than 10% in at least one histology and used for clustering four distinct histology types of B-lineage lymphomas. The frequency of each genetic lesion in each histology type is colour-coded. FL, follicular lymphoma; UPD, uniparental disomy. **b**, Recurrent genetic changes are depicted based on CNAG output of the SNP array analysis of 238 B-lineage lymphoma samples, which include gains at the *REL* locus on 2p16-15 (left panel) and the *A20* locus on 6q23.3 (right panel). Regions showing copy number gain or loss are indicated by horizontal lines. Four histology types are indicated by different colours, where high-grade amplifications and homozygous deletions are shown by darker shades to discriminate from simple gains (copy number ≤4) and losses (copy number = 1) (lighter shades). **c**, Point mutations and small nucleotide insertions and deletions in the *A20* (*TNFAIP3*) gene caused premature truncation of A20 in most cases. Altered amino acids caused by frame shifts are indicated by green bars.

genomic DNA was extracted from 150 microdissected CD30-positive tumour cells (Reed–Sternberg cells) for each sample. *A20* mutations were found in 18 out of 265 lymphoma samples (6.8%) (Table 1), among which 13 mutations, including nonsense mutations (3 cases), frame-shift insertions/deletions (9 cases), and a splicing donor site mutation (1 case) were thought to result in premature termination of translation (Fig. 1c). Four missense mutations and one intronic mutation were identified in five microdissected Hodgkin's lymphoma samples. They were not found in the surrounding normal tissues, and thus, were considered as tumour-specific somatic changes.

In total, biallelic *A20* lesions were found in 31 out of 265 lymphoma samples including 3 Hodgkin's lymphoma cell lines. Quantitative analysis of SNP array data suggested that these *A20* lesions were present in the major tumour fraction within the samples (Supplementary Fig. 7). Inactivation of *A20* was most frequent in MALT lymphoma (18 out of 87) and Hodgkin's lymphoma (7 out of 27), although it was also found in DLBCL (5 out of 64) and follicular lymphoma (1 out of 52) at lower frequencies. In MALT lymphoma, biallelic *A20* lesions were confirmed in 18 out of 24 cases (75.0%) with LOH involving the 6q23.3 segment (Supplementary Fig. 8). Considering the limitation in detecting very small homozygous deletions, *A20* was thought to be the target of 6q23 LOH in MALT lymphoma. On the other hand, the 6q23 LOHs in other histology types tended to be extended into more centromeric regions and less frequently accompanied biallelic *A20* lesions (Supplementary Fig. 8 and Supplementary Table 4), indicating that they might be more heterogeneous with regard to their gene targets. We were unable to analyse Hodgkin's lymphoma samples using SNP arrays owing to insufficient genomic DNA obtained from microdissected samples, and were likely to underestimate the frequency of *A20* inactivation in Hodgkin's lymphoma because we might fail to detect a substantial proportion of cases with homozygous deletions, which explained 50% (12 out of 24) of *A20* inactivation in other histology types. *A20* mutations in Hodgkin's lymphoma were exclusively found in nodular sclerosis classical Hodgkin's lymphoma (5 out of 15) but not in other histology types (0 out of 9), although the possible association requires further confirmation in additional cases.

A20 is a key regulator of NF-κB signalling, negatively modulating NF-κB activation through a wide variety of cell surface receptors and viral proteins, including tumour-necrosis factor (TNF) receptors, toll-like receptors, CD40, as well as Epstein–Barr-virus-associated LMP1 protein[2,5,17,18]. To investigate the role of A20 inactivation in lymphomagenesis, we re-expressed wild-type A20 under a *Tet*-inducible promoter in a lymphoma-derived cell line (KM-H2) that had no functional *A20* alleles (Supplementary Fig. 6), and examined the effect of A20 re-expression on cell proliferation, survival and downstream NF-κB signalling pathways. As shown in Fig. 2a–c and Supplementary Fig. 9, re-expression of wild-type A20 resulted in the suppression of cell proliferation and enhanced apoptosis, and in the concomitant accumulation of IκBβ and IκBε, and downregulation of NF-κB activity. In contrast, re-expression of two lymphoma-derived A20 mutants, $A20^{532Stop}$ or $A20^{750Stop}$, failed to show growth suppression, induction of apoptosis, accumulation of IκBβ and IκBε or downregulation of

Table 1 | Inactivation of A20 in B-lineage lymphomas

Histology	Tissue	Sample	Allele	Uniparental disomy	Exon	Mutation	Biallelic inactivation
DLBCL							5 out of 64 (7.8%)
	Lymph node	DLBCL008	−/−	No	–	–	
	Lymph node	DLBCL016	+/−	No	Ex2	329insA	
	Lymph node	DLBCL022	−/−	No	–	–	
	Lymph node	DLBCL028	−/−	Yes	–	–	
	Lymph node	MCL008*	−/−	Yes	–	–	
Follicular lymphoma							1 out of 52 (1.9%)
	Lymph node	FL024	−/−	No	–	–	
MCL							0 out of 35 (0%)
MALT							18 out of 87 (21.8%)
Stomach							3 out of 23 (13.0%)
	Gastric mucosa	MALT013	+/+	Yes	Ex5	705insG	
	Gastric mucosa	MALT014	+/+	Yes	Ex3	Ex3 donor site>A	
	Gastric mucosa	MALT036	+/−	No	Ex7	delintron6–Ex7†	
Eye							13 out of 43 (30.2%)
	Ocular adnexa	MALT008	−/−	No	–	–	
	Ocular adnexa	MALT017	−/−	No	–	–	
	Ocular adnexa	MALT051	+/−	No	Ex7	1943delTG	
	Ocular adnexa	MALT053	+/+	Yes	Ex6	1016G>A(stop)	
	Ocular adnexa	MALT054	+/−	No	Ex3	502delTC	
	Ocular adnexa	MALT055	−/−	No	–	–	
	Ocular adnexa	MALT066	+/−	No	Ex7	1581insA	
	Ocular adnexa	MALT067	−/−	No	–	–	
	Ocular adnexa	MALT082	−/−	Yes	–	–	
	Ocular adnexa	MALT084	−/−	Yes	–	–	
	Ocular adnexa	MALT085	+/+	Yes	Ex7	1435insG	
	Ocular adnexa	MALT086	+/+	Yes	Ex6	878C>T(stop)	
	Ocular adnexa	MALT087	+/+	Yes	Ex9	2304delGG	
Lung							2 out of 12 (16.7%)
	Lung	MALT042	−/−	No	–	–	
	Lung	MALT047	+/+	Yes	Ex9	2281insT	
Other‡							0 out of 9 (0%)
Hodgkin's lymphoma							7 out of 27 (26.0%)
NSHL	Lymph node	HL10	ND	ND	Ex7	1777G>A(V571I)	
NSHL	Lymph node	HL12	ND	ND	Ex7	1156A>G(R364G)	
NSHL	Lymph node	HL21	ND	ND	Ex4	569G>A(stop)	
NSHL	Lymph node	HL24	ND	ND	Ex3	1487C>A(T474N)	
NSHL	Lymph node	HL23	ND	ND	–	Intron 3§	
	Cell line	KM-H2	−/−	No	–		
	Cell line	HDLM2	+/−	No	Ex4	616ins29bp‖	
Total							31 out of 265 (11.7%)

DLBCL, diffuse large B-cell lymphoma; MALT, MALT lymphoma; MCL, mantle cell lymphoma; ND, not determined because SNP array analysis was not performed; NSHL, nodular sclerosis classical Hodgkin's lymphoma.
* Diagnosis was changed based on the genomic data, which was confirmed by re-examination of pathology.
† Deletion including the boundary of intron 6 and exon 7 (see also Supplementary Fig. 5b).
‡ Including 1 parotid gland, 1 salivary gland, 2 colon and 5 thyroid cases.
§ Insertion of CTC at −19 bases from the beginning of exon 3.
‖ Insertion of TGGCTTCCACAGACACACCCATGGCCCGA.

NF-κB activity (Fig. 2a–c), indicating that these were actually loss-of-function mutations. To investigate the role of A20 inactivation in lymphomagenesis *in vivo*, *A20*- and mock-transduced KM-H2 cells were transplanted in NOD/SCID/γ_c^{null} (NOG) mice[19], and their tumour formation status was examined for 5 weeks with or without induction of wild-type A20 by tetracycline administration. As shown in Fig. 2d, mock-transduced cells developed tumours at the injected sites, whereas the *Tet*-inducible *A20*-transduced cells generated tumours only in the absence of A20 induction (Supplementary Table 5), further supporting the tumour suppressor role of A20 in lymphoma development.

Given the mode of negative regulation of NF-κB signalling, we next investigated the origins of NF-κB activity that was deregulated by A20 loss in KM-H2 cells. The conditioned medium prepared from a 48-h serum-free KM-H2 culture had increased NF-κB upregulatory activity compared with fresh serum-free medium, which was inhibited by re-expression of A20 (Fig. 3a). KM-H2 cells secreted two known ligands for TNF receptor—TNF-α and lymphotoxin-α (Supplementary Fig. 10)[20]—and adding neutralizing antibodies against these cytokines into cultures significantly suppressed their cell growth and NF-κB activity without affecting the levels of their overall suppression after A20 induction (Fig. 3b, d). In addition, recombinant TNF-α and/or lymphotoxin-α added to fresh serum-free medium promoted cell growth and NF-κB activation in KM-H2 culture, which were again suppressed by re-expression of A20 (Fig. 3c, e). Although our data in Fig. 3 also show the presence of factors other than TNF-α and lymphotoxin-α in the KM-H2-conditioned medium—as well as some intrinsic pathways in the cell (Fig. 3a)—that were responsible for the A20-dependent NF-κB activation, these results indicate that both cell growth and NF-κB activity that were upregulated by A20 inactivation depend at least partly on the upstream stimuli that evoked the NF-κB-activating signals.

Aberrant activation of the NF-κB pathway is a hallmark of several subtypes of B-lineage lymphomas, including Hodgkin's lymphoma, MALT lymphoma, and a subset of DLBCL, as well as other lymphoid neoplasms[11,14], where a number of genetic alterations of NF-κB signalling pathway genes[21–25], as well as some viral proteins[26,27], have been implicated in the aberrant activation of the NF-κB pathway[14]. Thus, frequent inactivation of A20 in Hodgkin's lymphoma and MALT and other lymphomas provides a novel insight into the molecular pathogenesis of these subtypes of B-lineage lymphomas through deregulated NF-κB activation. Because A20 provides a

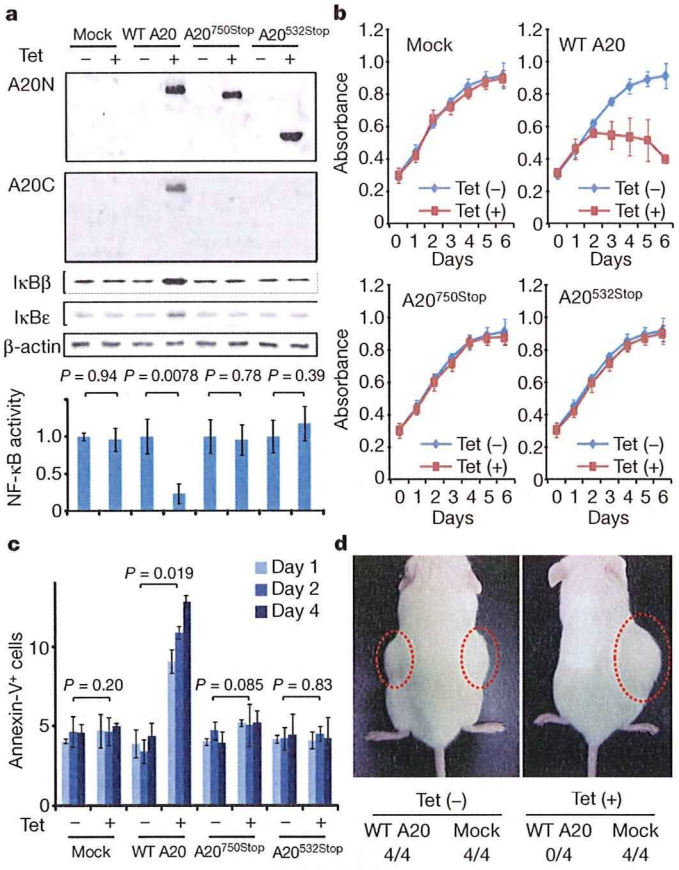

Figure 2 | Effects of wild-type and mutant A20 re-expressed in a lymphoma cell line that lacks the normal *A20* gene. a, Western blot analyses of wild-type (WT) and mutant ($A20^{532Stop}$ and $A20^{750Stop}$) A20, as well as IκBβ and IκBε, in KM-H2 cells, in the presence or absence of tetracycline treatment (top panels). A20N and A20C are polyclonal antisera raised against N-terminal and C-terminal A20 peptides, respectively. β-actin blots are provided as a control. NF-κB activities are expressed as mean absorbance ± s.d. ($n = 6$) in luciferase assays (bottom panel). **b,** Proliferation of KM-H2 cells stably transduced with plasmids for mock and *Tet*-inducible wild-type A20, $A20^{532Stop}$ and $A20^{750Stop}$ was measured using a cell counting kit in the presence (red lines) or absence (blue lines) of tetracycline. Mean absorbance ± s.d. ($n = 5$) is plotted. **c,** The fractions of Annexin-V-positive KM-H2 cells transduced with various *Tet*-inducible A20 constructs were measured by flow cytometry after tetracycline treatment and the mean values (±s.d., $n = 3$) are plotted. **d,** *In vivo* tumorigenicity was assayed by inoculating 7×10^6 KM-H2 cells transduced with mock or *Tet*-inducible wild-type A20 in NOG mice, with (right panel) or without (left panel) tetracycline administration.

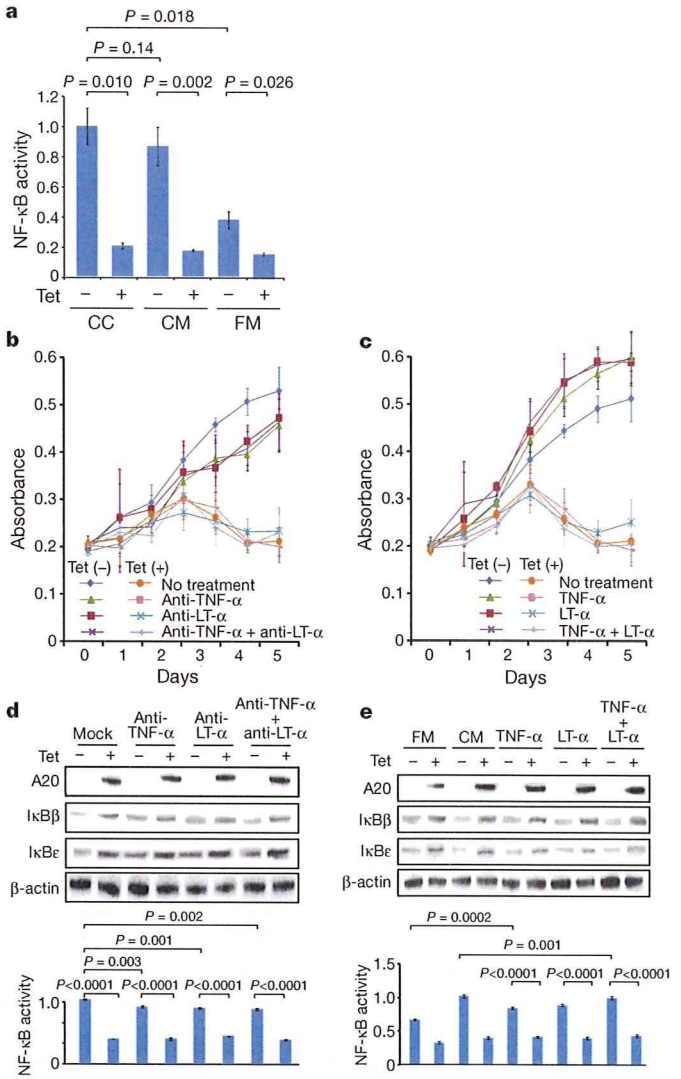

Figure 3 | Tumour suppressor role of A20 under external stimuli. a, NF-κB activity in KM-H2 cells was measured 30 min after cells were inoculated into fresh medium (FM) or KM-H2-conditioned medium (CM) obtained from the 48-h culture of KM-H2, and was compared with the activity after 48 h continuous culture of KM-H2 (CC). A20 was induced 12 h before inoculation in Tet (+) groups. **b, c,** Effects of neutralizing antibodies against TNF-α and lymphotoxin-α (LTα) (**b**) and of recombinant TNF-α and LT-α added to the culture (**c**) on cell growth were evaluated in the presence (Tet (+)) or absence (Tet (−)) of A20 induction. Cell numbers were measured using a cell counting kit and are plotted as their mean absorbance ± s.d. ($n = 6$). **d, e,** Effects of the neutralizing antibodies (**d**) and the recombinant cytokines added to the culture (**e**) on NF-κB activities and the levels of IκBβ and IκBε after 48 h culture with (Tet (+)) or without (Tet (−)) tetracycline treatment. NF-κB activities are expressed as mean absorbance ± s.d. ($n = 6$) in luciferase assays.

negative feedback mechanism in the regulation of NF-κB signalling pathways upon a variety of stimuli, aberrant activation of NF-κB will be a logical consequence of A20 inactivation. However, there is also the possibility that the aberrant NF-κB activity of A20-inactivated lymphoma cells is derived from upstream stimuli, which may be from the cellular environment. In this context, it is intriguing that MALT lymphoma usually arises at the site of chronic inflammation caused by infection or autoimmune disorders and may show spontaneous regression after eradication of infectious organisms[28]; furthermore, Hodgkin's lymphoma frequently shows deregulated cytokine production from Reed–Sternberg cells and/or surrounding reactive cells[29]. Detailed characterization of the NF-κB pathway regulated by A20 in both normal and neoplastic B lymphocytes will promote our understanding of the precise roles of A20 inactivation in the pathogenesis of these lymphoma types. Our finding underscores the importance of genome-wide approaches in the identification of genetic targets in human cancers.

METHODS SUMMARY

Genomic DNA from 238 patients with non-Hodgkin's lymphoma and three Hodgkin's-lymphoma-derived cell lines was analysed using GeneChip SNP genotyping microarrays (Affymetrix). This study was approved by the ethics boards of the University of Tokyo, National Cancer Institute Hospital, Okayama University, and the Cancer Institute of the Japanese Foundation of Cancer Research. After appropriate normalization of mean array intensities, signal ratios between tumours and anonymous normal references were calculated in an allele-specific manner, and allele-specific copy numbers were inferred from the observed signal ratios based on the hidden Markov model using CNAG/AsCNAR software (http://www.genome.umin.jp). *A20* mutations were examined by directly sequencing genomic DNA using a set of primers (Supplementary Table 6). Full-length cDNAs of wild-type and mutant *A20* were introduced into a

lentivirus vector, pLenti4/TO/V5-DEST (Invitrogen), with a *Tet*-inducible promoter. Viral stocks were prepared by transfecting the vector plasmids into 293FT cells (Invitrogen) using the calcium phosphate method and then infected to the KM-H2 cell line. Proliferation of KM-H2 cells was measured using a Cell Counting Kit (Dojindo). Western blot analyses and luciferase assays were performed as previously described. NF-κB activity was measured by luciferase assays in KM-H2 cells stably transduced with a reporter plasmid having an NF-κB response element, pGL4.32 (Promega). Apoptosis of KM-H2 upon A20 induction was evaluated by counting Annexin-V-positive cells by flow cytometry. For *in vivo* tumorigenicity assays, 7×10^6 KM-H2 cells were transduced with the *Tet*-inducible *A20* gene and those with a mock vector were inoculated on the contralateral sides in eight NOG mice[19] and examined for their tumour formation with ($n = 4$) or without ($n = 4$) tetracycline administration. Full copy number data of the 238 lymphoma samples will be accessible from the Gene Expression Omnibus (GEO, http://ncbi.nlm.nih.gov/geo/) with the accession number GSE12906.

Full Methods and any associated references are available in the online version of the paper at www.nature.com/nature.

Received 17 September 2008; accepted 3 March 2009.
Published online 3 May 2009.

1. Dixit, V. M. *et al.* Tumor necrosis factor-α induction of novel gene products in human endothelial cells including a macrophage-specific chemotaxin. *J. Biol. Chem.* **265,** 2973–2978 (1990).
2. Song, H. Y., Rothe, M. & Goeddel, D. V. The tumor necrosis factor-inducible zinc finger protein A20 interacts with TRAF1/TRAF2 and inhibits NF-κB activation. *Proc. Natl Acad. Sci. USA* **93,** 6721–6725 (1996).
3. Lee, E. G. *et al.* Failure to regulate TNF-induced NF-κB and cell death responses in A20-deficient mice. *Science* **289,** 2350–2354 (2000).
4. Boone, D. L. *et al.* The ubiquitin-modifying enzyme A20 is required for termination of Toll-like receptor responses. *Nature Immunol.* **5,** 1052–1060 (2004).
5. Wang, Y. Y., Li, L., Han, K. J., Zhai, Z. & Shu, H. B. A20 is a potent inhibitor of TLR3- and Sendai virus-induced activation of NF-κB and ISRE and IFN-β promoter. *FEBS Lett.* **576,** 86–90 (2004).
6. Wertz, I. E. *et al.* De-ubiquitination and ubiquitin ligase domains of A20 downregulate NF-κB signalling. *Nature* **430,** 694–699 (2004).
7. Heyninck, K. & Beyaert, R. A20 inhibits NF-κB activation by dual ubiquitin-editing functions. *Trends Biochem. Sci.* **30,** 1–4 (2005).
8. Graham, R. R. *et al.* Genetic variants near *TNFAIP3* on 6q23 are associated with systemic lupus erythematosus. *Nature Genet.* **40,** 1059–1061 (2008).
9. Musone, S. L. *et al.* Multiple polymorphisms in the *TNFAIP3* region are independently associated with systemic lupus erythematosus. *Nature Genet.* **40,** 1062–1064 (2008).
10. Jaffe, E. S., Harris, N. L., Stein, H. & Vardiman, J. W. *World Health Organization Classification of Tumours. Pathology and Genetics of Tumours of Hematopoietic and Lymphoid Tissues* (IARC Press, 2001).
11. Klein, U. & Dalla-Favera, R. Germinal centres: role in B-cell physiology and malignancy. *Nature Rev. Immunol.* **8,** 22–33 (2008).
12. Nannya, Y. *et al.* A robust algorithm for copy number detection using high-density oligonucleotide single nucleotide polymorphism genotyping arrays. *Cancer Res.* **65,** 6071–6079 (2005).
13. Yamamoto, G. *et al.* Highly sensitive method for genomewide detection of allelic composition in nonpaired, primary tumor specimens by use of affymetrix single-nucleotide-polymorphism genotyping microarrays. *Am. J. Hum. Genet.* **81,** 114–126 (2007).
14. Jost, P. J. & Ruland, J. Aberrant NF-κB signaling in lymphoma: mechanisms, consequences, and therapeutic implications. *Blood* **109,** 2700–2707 (2007).
15. Durkop, H., Hirsch, B., Hahn, C., Foss, H. D. & Stein, H. Differential expression and function of A20 and TRAF1 in Hodgkin lymphoma and anaplastic large cell lymphoma and their induction by CD30 stimulation. *J. Pathol.* **200,** 229–239 (2003).
16. Honma, K. *et al. TNFAIP3* is the target gene of chromosome band 6q23.3-q24.1 loss in ocular adnexal marginal zone B cell lymphoma. *Genes Chromosom. Cancer* **47,** 1–7 (2008).
17. Sarma, V. *et al.* Activation of the B-cell surface receptor CD40 induces A20, a novel zinc finger protein that inhibits apoptosis. *J. Biol. Chem.* **270,** 12343–12346 (1995).
18. Fries, K. L., Miller, W. E. & Raab-Traub, N. The A20 protein interacts with the Epstein-Barr virus latent membrane protein 1 (LMP1) and alters the LMP1/TRAF1/TRADD complex. *Virology* **264,** 159–166 (1999).
19. Hiramatsu, H. *et al.* Complete reconstitution of human lymphocytes from cord blood $CD34^+$ cells using the NOD/SCID/γ^{null} mice model. *Blood* **102,** 873–880 (2003).
20. Hsu, P. L. & Hsu, S. M. Production of tumor necrosis factor-α and lymphotoxin by cells of Hodgkin's neoplastic cell lines HDLM-1 and KM-H2. *Am. J. Pathol.* **135,** 735–745 (1989).
21. Dierlamm, J. *et al.* The apoptosis inhibitor gene *API2* and a novel 18q gene, *MLT*, are recurrently rearranged in the t(11;18)(q21;q21) associated with mucosa-associated lymphoid tissue lymphomas. *Blood* **93,** 3601–3609 (1999).
22. Willis, T. G. *et al.* Bcl10 is involved in t(1;14)(p22;q32) of MALT B cell lymphoma and mutated in multiple tumor types. *Cell* **96,** 35–45 (1999).
23. Joos, S. *et al.* Classical Hodgkin lymphoma is characterized by recurrent copy number gains of the short arm of chromosome 2. *Blood* **99,** 1381–1387 (2002).
24. Martin-Subero, J. I. *et al.* Recurrent involvement of the *REL* and *BCL11A* loci in classical Hodgkin lymphoma. *Blood* **99,** 1474–1477 (2002).
25. Lenz, G. *et al.* Oncogenic *CARD11* mutations in human diffuse large B cell lymphoma. *Science* **319,** 1676–1679 (2008).
26. Deacon, E. M. *et al.* Epstein-Barr virus and Hodgkin's disease: transcriptional analysis of virus latency in the malignant cells. *J. Exp. Med.* **177,** 339–349 (1993).
27. Yin, M. J. *et al.* HTLV-I Tax protein binds to MEKK1 to stimulate IκB kinase activity and NF-κB activation. *Cell* **93,** 875–884 (1998).
28. Isaacson, P. G. & Du, M. Q. MALT lymphoma: from morphology to molecules. *Nature Rev. Cancer* **4,** 644–653 (2004).
29. Skinnider, B. F. & Mak, T. W. The role of cytokines in classical Hodgkin lymphoma. *Blood* **99,** 4283–4297 (2002).

Supplementary Information is linked to the online version of the paper at www.nature.com/nature.

Acknowledgements This work was supported by the Core Research for Evolutional Science and Technology, Japan Science and Technology Agency, by the 21st century centre of excellence program 'Study on diseases caused by environment/genome interactions', and by Grant-in-Aids from the Ministry of Education, Culture, Sports, Science and Technology of Japan and from the Ministry of Health, Labor and Welfare of Japan for the 3rd-term Comprehensive 10-year Strategy for Cancer Control. We also thank Y. Ogino, E. Matsui and M. Matsumura for their technical assistance.

Author Contributions M.Ka., K.N. and M.S. performed microarray experiments and subsequent data analyses. M.Ka., Y.C., K.Ta., J.T., J.N., M.I., A.T. and Y.K. performed mutation analysis of *A20*. M.Ka., S.Mu., M.S., Y.C. and Y.Ak. conducted functional assays of mutant A20. Y.S., K.Ta., Y.As., H.M., M.Ku., S.Mo., S.C., Y.K., K.To. and Y.I. prepared tumour specimens. I.K., K.O., A.N., H.N. and T.N. conducted *in vivo* tumorigenicity experiments in NOG/SCID mice. T.I., Y.H., T.Y., Y.K. and S.O. designed overall studies, and S.O. wrote the manuscript. All authors discussed the results and commented on the manuscript.

Author Information The copy number data as well as the raw microarray data will be accessible from the GEO (http://ncbi.nlm.nih.gov/geo/) with the accession number GSE12906. Reprints and permissions information is available at www.nature.com/reprints. Correspondence and requests for materials should be addressed to S.O. (sogawa-tky@umin.ac.jp) or Y.K. (ykkobaya@ncc.go.jp).

METHODS

Specimens. Primary tumour specimens were obtained from patients who were diagnosed with DLBCL, follicular lymphoma, MCL, MALT lymphoma, or classical Hodgkin's lymphoma. In total, 238 primary lymphoma specimens listed in Supplementary Table 1 were subjected to SNP array analysis. Three Hodgkin's-lymphoma-derived cell lines (KM-H2, HDLM2, L540) were obtained from Hayashibara Biochemical Laboratories, Inc., Fujisaki Cell Center and were also analysed by SNP array analysis.

Microarray analysis. High-molecular-mass DNA was isolated from tumour specimens and subjected to SNP array analysis using GeneChip Mapping 50K and/or 250K arrays (Affymetrix). The scanned array images were processed with Gene Chip Operation software (GCOS), followed by SNP calls using GTYPE. Genome-wide copy number measurements and LOH detection were performed using CNAG/AsCNAR software[12,13].

Mutation analysis. Mutations in the *A20* gene were examined in 265 samples of B-lineage lymphoma, including 62 DLBCLs, 52 follicular lymphomas, 87 MALTs, 37 MCLs and 3 Hodgkin's-lymphoma-derived cell lines and 24 primary Hodgkin's lymphoma samples, by direct sequencing using an ABI PRISM 3130xl Genetic Analyser (Applied Biosystems). To analyse primary Hodgkin's lymphoma samples in which CD30-positive tumour cells (Reed–Sternberg cells) account for only a fraction of the specimen, 150 Reed–Sternberg cells were collected for each 10 μm slice of a formalin-fixed block immunostained for CD30 by laser-capture microdissection (ASLMD6000, Leica), followed by genomic DNA extraction using QIAamp DNA Micro kit (Qiagen). The primer sets used in this study are listed in Supplementary Table 6.

Functional analysis of wild-type and mutant A20. Full-length cDNA for wild-type *A20* was isolated from total RNA extracted from an acute myeloid leukaemia-derived cell line, CTS, and subcloned into a lentivirus vector (pLenti4/TO/V5-DEST, Invitrogen). cDNAs for mutant A20 were generated by PCR amplification using mutagenic primers (Supplementary Table 6), and introduced into the same lentivirus vector. Forty-eight hours after transfection of each plasmid into 293FT cells using the calcium phosphate method, lentivirus stocks were obtained from ultrafiltration using Amicon Ultra (Millipore), and used to infect KM-H2 cells to generate stable transfectants of mock, wild-type and mutant A20. Each KM-H2 derivative cell line was further transduced stably with a reporter plasmid (pGL4.32, Promega) containing a luciferase gene under an NF-κB-responsive element by electroporation using Nucleofector reagents (Amaxa).

Assays for cell proliferation and NF-κB activity. Proliferation of the KM-H2 derivative cell lines was assayed in triplicate using a Cell Counting Kit (Dojindo). The mean absorption of five independent assays was plotted with s.d. for each derivative line. Two independent KM-H2-derived cell lines were used for each experiment. The NF-κB activity in KM-H2 derivatives for A20 mutants was evaluated by luciferase assays using a PiccaGene Luciferase Assay Kit (TOYO B-Net Co.). Each assay was performed in triplicate and the mean absorption of five independent experiments was plotted with s.d.

Western blot analyses. Polyclonal anti-sera against N-terminal (anti-A20N) and C-terminal (anti-A20C) A20 peptides were generated by immunizing rabbits with these peptides (LSNMRKAVKIRERTPEDIC for anti-A20N and CFQFKQMYG for anti-A20C, respectively). Total cell lysates from KM-H2 cells were separated on 7.5% polyacrylamide gel and subjected to western blot analysis using antibodies to A20 (anti-A20N and anti-A20C), IκBα (sc-847), IκBβ (sc-945), IκBγ (sc-7155) and actin (sc-8432) (Santa Cruz Biotechnology).

Functional analyses of wild-type and mutant A20. Each KM-H2 derivative cell line stably transduced with various *Tet*-inducible A20 constructs was cultured in serum-free medium in the presence or absence of A20 induction using 1 μg ml^{-1} of tetracycline, and cell number was counted every day. 1×10^6 cells of each KM-H2 derivative cell line were analysed for their intracellular levels of IκBβ and IκBε and for NF-κB activities by western blot analyses and luciferase assays, respectively, 12 h after the beginning of cell culture. Effects of human recombinant TNF-α and lymphotoxin-α (210-TA and 211-TB, respectively, R&D Systems) on the NF-κB pathway and cell proliferation were evaluated by adding both cytokines into 10 ml of serum-free cell culture at a concentration of 200 pg ml^{-1}. For cell proliferation assays, culture medium was half replaced every 12 h to minimize the side-effects of autocrine cytokines. Intracellular levels of IκBβ, IκBε and NF-κB were examined 12 h after the beginning of the cell culture. To evaluate the effect of neutralizing TNF-α and lymphotoxin-α, 1×10^6 of KM-H2 cells transduced with both *Tet*-inducible A20 and the NF-κB-luciferase reporter were pre-cultured in serum-free media for 36 h, and thereafter neutralizing antibodies against TNF-α (MAB210, R&D Systems) and/or lymphotoxin-α (AF-211-NA, R&D Systems) were added to the media at a concentration of 200 pg ml^{-1}. After the extended culture during 12 h with or without 1 μg ml^{-1} tetracycline, the intracellular levels of IκBβ and IκBε and NF-κB activities were examined by western blot analysis and luciferase assays, respectively. To examine the effects of A20 re-expression on apoptosis, 1×10^6 KM-H2 cells were cultured for 4 days in 10 ml medium with or without *Tet* induction. After staining with phycoerythrin-conjugated anti-Annexin-V (ID556422, Becton Dickinson), Annexin-V-positive cells were counted by flow cytometry at the indicated times.

***In vivo* tumorigenicity assays.** KM-H2 cells transduced with a mock or *Tet*-inducible wild-type *A20* gene were inoculated into NOG mice and their tumorigenicity was examined for 5 weeks with or without tetracycline administration. Injections of 7×10^6 cells of each KM-H2 cell line were administered to two opposite sites in four mice. Tetracycline was administered in drinking water at a concentration of 200 μg ml^{-1}.

ELISA. Concentrations of TNF-α, lymphotoxin-α, IL-1, IL-2, IL-4, IL-6, IL-12, IL-18 and TGF-β in the culture medium were measured after 48 h using ELISA. For those cytokines detectable after 48-h culture (TNFα, LTα, and IL-6), their time course was examined further using the Quantikine ELISA kit (R&D Systems).

Statistical analysis. Significance of the difference in NF-κB activity between two given groups was evaluated using a paired *t*-test, in which the data from each independent luciferase assay were paired to calculate test statistics. To evaluate the effect of A20 re-expression in KM-H2 cells on apoptosis, the difference in the fractions of Annexin-V-positive cells between Tet (+) and Tet (−) groups was also tested by a paired *t*-test for assays, in which the data from the assays performed on the same day were paired.

Aurora-A kinase: a novel target of cellular immunotherapy for leukemia

Toshiki Ochi,[1] Hiroshi Fujiwara,[1] Koichiro Suemori,[1] Taichi Azuma,[1] Yoshihiro Yakushijin,[2] Takaaki Hato,[3] Kiyotaka Kuzushima,[4] and Masaki Yasukawa[1,5]

[1]Department of Bioregulatory Medicine, [2]Cancer Center, and [3]Division of Blood Transfusion and Cell Therapy, Ehime University Graduate School of Medicine, Toon; [4]Division of Immunology, Aichi Cancer Center, Nagoya; and [5]Center for Regenerative Medicine, Ehime University Graduate School of Medicine, Toon, Japan

Aurora-A kinase (Aur-A) is a member of the serine/threonine kinase family that regulates the cell division process, and has recently been implicated in tumorigenesis. In this study, we identified an antigenic 9–amino-acid epitope (Aur-$A_{207-215}$: YLILEYAPL) derived from Aur-A capable of generating leukemia-reactive cytotoxic T lymphocytes (CTLs) in the context of HLA-A*0201. The synthetic peptide of this epitope appeared to be capable of binding to HLA-A*2402 as well as HLA-A*0201 molecules. Leukemia cell lines and freshly isolated leukemia cells, particularly chronic myelogenous leukemia (CML) cells, appeared to express Aur-A abundantly. Aur-A–specific CTLs were able to lyse human leukemia cell lines and freshly isolated leukemia cells, but not normal cells, in an HLA-A*0201–restricted manner. Importantly, Aur-A–specific CTLs were able to lyse CD34$^+$ CML progenitor cells but did not show any cytotoxicity against normal CD34$^+$ hematopoietic stem cells. The tetramer assay revealed that the Aur-$A_{207-215}$ epitope–specific CTL precursors are present in peripheral blood of HLA-A*0201–positive and HLA-A*2402–positive patients with leukemia, but not in healthy individuals. Our results indicate that cellular immunotherapy targeting Aur-A is a promising strategy for treatment of leukemia. (Blood. 2009;113: 66-74)

Introduction

Cellular immunotherapy for malignancies targeting various tumor-associated antigens has been developed.[1,2] Recently, some attractive target antigens recognized by leukemia-reactive cytotoxic T lymphocytes (CTLs), such as WT1 and PR1, have been discovered and phase 1/2 clinical studies of cancer immunotherapy targeting these antigens have been conducted; however, the clinical response against hematologic malignancies remains unsatisfactory.[3,4] To establish effective cancer immunotherapy, identification of target antigens that are recognized efficiently by tumor-specific CTLs is necessary. Antigens that can serve as ideal targets recognizable by tumor-specific CTLs need to have several essential characteristics. First, their expression should be limited to, or abundant in, tumor cells rather than normal cells. Second, the antigens should be efficiently processed in tumor cells and expressed on the cell surface in context with common HLA molecules. Third, target antigens should play an important role in tumorigenesis and/or progression of malignancies, because their expression is essential for tumor survival.

Aurora-A kinase (Aur-A) is a member of the serine/threonine kinase family, and the *Aur-A* gene is located at chromosome 20q13, a region frequently amplified in breast cancer.[5] Aur-A is mainly expressed in the G_2/M phase of the cell cycle and regulates mitotic cell division in normal cells.[6-8] Among normal tissues, Aur-A is expressed exclusively in testis, but in various kinds of cancer it is aberrantly overexpressed, and associated with poor prognosis.[9-14] Overexpression of Aur-A determined by amplification of *Aur-A* mRNA has also been widely observed in hematologic malignancies.[15-19] Aur-A overexpression has been linked with centrosome amplification, aneuploidy, and chromosome instability.[20,21] Furthermore, ectopic overexpression of Aur-A efficiently transforms immortalized rodent fibroblasts.[9,20] These data strongly suggest that *Aur-A* is one of the fundamental cancer-associated genes and a potential target for cancer treatment. In addition, previous reports have demonstrated that silencing of the gene encoding Aur-A in cancer cells results in inhibition of their growth and enhancement of the cytotoxic effect of anticancer agents.[22] Therefore the development of small molecules with an Aur-A–inhibitory function may make it possible to reduce or block the oncogenic activity of Aur-A. On the basis of this concept, clinical studies using Aur-A inhibitors for cancer treatment are now under way; however, their clinical efficacy is still unknown.[23-27] The biologic characteristics of Aur-A mentioned above suggest that it is an ideal target for tumor-specific CTLs, and that cancer immunotherapy targeting Aur-A could be feasible. In this study, therefore, we attempted to verify the feasibility of cellular immunotherapy for leukemia targeting Aur-A.

Methods

Synthetic peptides

Candidate peptides derived from Aur-A with high binding affinity for the HLA-A*0201 or HLA-A*2402 molecule were predicted algorithmically by the BIMAS program (http://www-bimas.cit.nih.gov/molbio/hla_bind/). On the basis of these data, peptides with favorable binding affinity for the HLA-A*0201 or HLA-A*2402 molecule were selected and synthesized (Thermo Electron; Greiner Bio-One, Tokyo, Japan). Amino acid sequences

Submitted June 24, 2008; accepted September 6, 2008. Prepublished online as *Blood* First Edition paper, September 26, 2008; DOI 10.1182/blood-2008-06-164889.

The online version of this article contains a data supplement.

The publication costs of this article were defrayed in part by page charge payment. Therefore, and solely to indicate this fact, this article is hereby marked "advertisement" in accordance with 18 USC section 1734.

Table 1. Binding affinities of synthetic peptides

HLA	Position	Length, mer	Sequence	Score	Fluorescence index
A*0201	Aur-$A_{271-279}$	9	KIADFGWSV	3911	0.93
A*0201	Aur-A_{63-71}	9	KLVSSHKPV	243	0.23
A*0201	Aur-$A_{207-215}$	9	YLILEYAPL	147	1.47
A*0201	$WT1_{7-15}$	9	DLNALLPAV	12	0.06
A*0201	$CMVpp65_{495-503}$	9	NLVPMVATV	160	1.71
A*2402	Aur-$A_{207-215}$	9	YLILEYAPL	6	0.99
A*2402	$WT1_{7-15}$	9	DLNALLPAV	0.18	0.02
A*2402	$WT1_{235-243}Y$	9	CYTWNQMNL	200	4.5

The binding affinities of synthetic peptides for HLA molecules were predicted by computer algorithms available on the National Institutes of Health BIMAS website (http://www-bimas.cit.nih.gov/molbio/hla_bind). The binding affinities of synthetic peptides for HLA molecules were evaluated by MHC stabilization assay as detailed in "HLA peptide–binding assay."

of the peptides used in this study are listed in Table 1. All the peptides were synthesized with a purity exceeding 80%.

HLA peptide–binding assay

Binding affinity of peptides for the HLA-A*0201 or HLA-A*2402 molecule was assessed by an HLA-A*0201 or HLA-A*2402 stabilization assay as described previously.[28,29] Briefly, the HLA-A*0201–positive cell line (T2) or the *HLA-A*2402* gene–transfected T2 cell line (T2-A24) was plated in 24-well plates at 10^6 cells per well and incubated overnight with the candidate peptides at a concentration of 10 μM in serum-free RPMI 1640 medium. The T2 and T2-A24 cells were washed twice with phosphate-buffered saline (PBS), and then incubated with fluorescein isothiocyanate (FITC)–conjugated anti–HLA-A2 or HLA-A24 monoclonal antibody (MoAb; One Lambda, Canoga Park, CA) at 4°C for 20 minutes. The cells were washed and suspended in 1 mL PBS and analyzed using a flow cytometer (FACSCalibur; Becton Dickinson, San Jose, CA). Measurement of mean fluorescence intensity and analysis of data were done with CellQuest Software (Becton Dickinson). The fluorescence index (FI) was calculated as FI = (sample mean − background mean) / background mean.

Cell lines, freshly isolated leukemia cells, and normal cells

Approval for this study was obtained from the institutional review board of Ehime University Hospital. Written informed consent was obtained from all patients, healthy volunteers, and parents of cord blood donors in accordance with the Declaration of Helsinki.

B-lymphoblastoid cell lines (B-LCLs) were established by transformation of peripheral blood B lymphocytes with Epstein-Barr virus. LCLs, T2, T2-A24, and leukemia cell lines were cultured in RPMI 1640 medium supplemented with 10% fetal calf serum (FCS). The *HLA-A*0201* gene–transfected C1R cell line (C1R-A*0201; kindly provided by Dr A. John Barrett, National Heart, Lung, and Blood Institute [NHLBI], Bethesda, MD) was cultured in RPMI 1640 medium supplemented with 10% FCS and 2 mM L-glutamine. Peripheral blood mononuclear cells (PBMCs) and bone marrow mononuclear cells (BMMCs) from leukemia patients and healthy volunteers, and cord blood mononuclear cells (CBMCs) from healthy donors were isolated and stored in liquid nitrogen until use. All leukemia samples contained more than 95% leukemia cells. $CD34^+$ cells from BMMCs and CBMCs were isolated using $CD34^+$ cell-isolating immunomagnetic beads (MACS beads; Miltenyi Biotec, Auburn, CA). In some experiments, BMMCs and CBMCs were stained with FITC-conjugated anti-CD34 MoAb and phycoerythrin (PE)–conjugated anti-CD38 MoAb, and $CD34^+CD38^{high}$ cells and $CD34^+CD38^{low}$ cells were sorted with an EPICS ALTRA cell sorter (Beckman-Coulter, Fullerton, CA).

Generation of Aur-A peptide–specific CTL lines

Aur-A peptide–specific CTLs were generated as described previously.[30] Briefly, monocytes ($CD14^+$ mononuclear cells) were isolated from PBMCs of HLA-A*0201–positive individuals using $CD14^+$ cell-isolating MACS beads. Monocytes were cultured in RPMI 1640 medium supplemented with 10% FCS, 75 ng/mL recombinant human granulocyte-macrophage colony-stimulating factor, 10 ng/mL recombinant human interleukin 4 (IL-4; R&D Systems, Minneapolis, MN), and 100 U/mL recombinant human tumor necrosis factor-α (Dainippon Pharmaceutical, Osaka, Japan) to generate mature dendritic cells (DCs). $CD8^+$ T lymphocytes isolated from PBMCs using $CD8^+$ cell-isolating MACS beads were plated in 96-well round-bottomed plates at 10^5 cells per well and stimulated with 10^4 autologous DCs pulsed with synthetic peptide derived from Aur-A at a concentration of 10 μM. The cells were cultured in RPMI 1640 medium supplemented with 10% human AB serum. After 7 days, the cells were restimulated with 10^4 autologous DCs pulsed with Aur-A peptide, and 10 U/mL IL-2 (Boehringer Mannheim, Mannheim, Germany) was added 4 days later. After culturing for a further 3 days (day 15 of culture), the cells were stimulated with 10^5 autologous PBMCs treated with mitomycin C (MMC; Kyowa Hakko, Tokyo, Japan) pulsed with Aur-A peptide. Thereafter, the cells were restimulated weekly by MMC-treated autologous PBMCs pulsed with Aur-A peptide. The Aur-A peptide–specific cytotoxic activity of growing cells was examined by standard ^{51}Cr-release assay.

Cytotoxicity assays

The standard ^{51}Cr-release assays were performed as described previously.[31] Briefly, 10^4 ^{51}Cr-labeled ($Na_2{}^{51}CrO_4$; New England Nuclear, Boston, MA) target cells and various numbers of effector cells in 200 μL RPMI 1640 medium supplemented with 10% FCS were seeded into 96-well round-bottom plates. The target cells were incubated with or without synthetic peptide for 2 hours before adding the effector cells. To assess the HLA class I restriction of cytotoxicity, target cells were incubated with an anti–HLA class I framework MoAb (w6/32; ATCC, Manassas, VA) or an anti–HLA-DR MoAb (L243; ATCC) at an optimal concentration (10 μg/mL) for 1 hour before adding the effector cells. Aur-A peptide specificity of cytotoxicity was examined by cold target inhibition assay as follows. ^{51}Cr-labeled target cells (hot targets) were mixed with various numbers of ^{51}Cr-unlabeled Aur-A peptide–loaded HLA-A*0201–positive LCLs or with ^{51}Cr-unlabeled Aur-A peptide–loaded HLA-A*0201–negative LCLs (cold targets). After incubation with the effector cells for 5 hours, 100 μL supernatant was collected from each well. The percentage of specific lysis was calculated as: (experimental release cpm − spontaneous release cpm) / (maximal release cpm − spontaneous release cpm) × 100 (%).

Quantitative analysis of *Aur-A* mRNA expression

Total RNA was extracted from each sample with an RNeasy Mini Kit (QIAGEN, Hilden, Germany) in accordance with the manufacturer's instructions. Quantitative real-time polymerase chain reaction (QRT-PCR) of *Aur-A* mRNA (Hs00269212_m1) and *glyceraldehyde-3-phosphate dehydrogenase* (*GAPDH*) mRNA (4326317E) as an internal control was performed using the TaqMan Gene Expression assay (Applied Biosystems, Foster City, CA) in accordance with the manufacturer's instructions using an ABI Prism 7700 Sequence Detection System (Applied Biosystems). The expression level of *Aur-A* mRNA was corrected by reference to that of *GAPDH* mRNA, and the relative amount of *Aur-A* mRNA in each sample was calculated by the comparative ΔCt method.